

# Genome wide analysis and comparative docking studies of new diaryl furan derivatives against human cyclooxygenase-2, lipoxygenase, thromboxane synthase and prostacyclin synthase enzymes involved in inflammatory pathway

P. Nataraj Sekhar<sup>a</sup>, L. Ananda Reddy<sup>a,\*</sup>, Marc De Maeyer<sup>b</sup>, K. Praveen Kumar<sup>c</sup>, Y.S. Srinivasulu<sup>c</sup>, M.S.L. Sunitha<sup>a</sup>, I.S.N. Sphoorthi<sup>d</sup>, G. Jayasree<sup>d</sup>, A. Maruthi Rao<sup>e</sup>, V.S. Kothekar<sup>f</sup>, P.V.B.S. Narayana<sup>g</sup>, P.B. Kavi Kishor<sup>a</sup>

<sup>a</sup> Department of Genetics, Osmania University, Hyderabad 500 007, India

<sup>b</sup> Laboratory of Biomolecular Modelling, Division Biochemistry, Molecular and Structural Biology, Department of Chemistry, Katholieke University, Leuven, Belgium

<sup>c</sup> Sri Venkateswara University, Tirupathi 517 501, India

<sup>d</sup> Srinidhi Institute of Science and Technology, Hyderabad 500 007, India

<sup>e</sup> Department of Botany, Telangana University, Nizamabad 503 002, India

<sup>f</sup> Department of Botany, Dr. B.A.M. University, Aurangabad 431 004, India

<sup>g</sup> CARISM, SASTRA University, Thanjavur, India

## ARTICLE INFO

### Article history:

Received 20 April 2009

Received in revised form 19 August 2009

Accepted 20 August 2009

Available online 27 August 2009

### Keywords:

COX-2

Thromboxane synthase

Lipoxygenase

Homology modelling

Docking

## ABSTRACT

In an effort to develop potent anti-inflammatory and antithrombotic drugs, a series of new 4-(2-phenyltetrahydrofuran-3-yl) benzene sulfonamide analogs were designed and docked against homology models of human cyclooxygenase-2 (COX-2), lipoxygenase and thromboxane synthase enzymes built using MODELLER 7v7 software and refined by molecular dynamics for 2 ns in a solvated layer. Validation of these homology models by procheck, verify-3D and ERRAT programs revealed that these models are highly reliable. Docking studies of 4-(2-phenyltetrahydrofuran-3-yl) benzene sulfonamide analogs designed by substituting different chemical groups on benzene rings replacing 1H pyrazole in celecoxib with five membered thiophene, furan, 1H pyrrole, 1H imidazole, thiazole and 1,3-oxazole showed that diaryl furan molecules showed good binding affinity towards mouse COX-2. Further, docking studies of diaryl furan derivatives are likely to have superior thromboxane synthase and COX-2 selectivity. Docking studies against site directed mutagenesis of Arg120Ala, Ser530Ala, Ser530Met and Tyr355Phe enzymes displayed the effect of inhibition of COX-2. Drug likeliness and activity decay for these inhibitors showed that these molecules act as best drugs at very low concentrations.

© 2009 Elsevier Inc. All rights reserved.

## 1. Introduction

Cyclooxygenase-2 (COX-2) is an important enzyme responsible for the formation of biological mediators called prostanoids [1] including prostaglandins (PGs), prostacyclins and thromboxanes [2]. PGs are ubiquitous fatty-acid derivatives that serve as autocrine/paracrine mediators involved in many different physiological processes. Non-steroidal antiinflammatory drugs and COX-2 inhibitors bind to COX-2 and provide relief from the symptoms of pain and inflammation. COX converts arachidonic acid (AA, a  $\omega$ -6 essential fatty acid) to prostaglandin H<sub>2</sub> (PGH<sub>2</sub>), the precursor of the series-2 prostanoids [3]. The resulting PGH<sub>2</sub> acts as a substrate

for isomerase pathways that produce other PG, thromboxane, and prostacyclin isomers. The enzyme contains two active sites: a heme with peroxidase activity, responsible for the reduction of PGG<sub>2</sub> to PGH<sub>2</sub>, and a cyclooxygenase active site, binds arachidonic acid, cyclizes and oxygenates it to form an unstable intermediate PGG<sub>2</sub>. This short-lived molecule diffuses from the COX active site to the peroxidase active site, where a hydroperoxyl moiety on PGG<sub>2</sub> is reduced to a hydroxyl. The resulting PGH<sub>2</sub> acts as a substrate for isomerase pathways that produce other PG, thromboxane, and prostacyclin isomers. The enzyme exists in two forms, COX-1 and COX-2. COX-1 is constitutively expressed and COX-2 is inducible. Both these enzymes show 60% homology with the same catalytic site, except that isoleucine at position 523 in COX-1 is replaced with valine in COX-2 responsible for hydrophobic side pocket in the enzyme. Both the isoenzymes are homodimers with distinct domains for dimerization,

\* Corresponding author. Tel.: +91 40 2768 2335; fax: +91 40 2709 5178.

E-mail address: [lakkireddy\\_anandareddy@rediffmail.com](mailto:lakkireddy_anandareddy@rediffmail.com) (L.A. Reddy).

membrane binding and catalysis. Recent studies indicate that COX-1 utilizes arginine120 in its active site to form an ionic bond with the carboxylate group of arachidonate. Conversely, arginine120 appears to form a hydrogen bond with arachidonate in the COX-2 active site, and this interaction contributes less to the binding energy than the ionic bond formation does in COX-1 [4]. This and other subtle differences in the COX-2 active site were exploited to produce COX-2 selective inhibitors.

### 1.1. Lipoxygenases, thromboxane synthase and prostacyclin synthase

Lipoxygenases possess regiospecificity during interaction with substrates and on this basis were designated as arachidonate 5-, 8-, 12-, 15-lipoxygenases (5-LOX, 8-LOX, 12-LOX, and 15-LOX) [1,5–9]. The four distinct enzymes insert oxygen at carbon 5, 8, 12 or 15 of arachidonic acid. The primary products are 5S-, 8S-, 12S-, or 15S-hydroperoxyeicosatetraenoic acid (5-, 8-, 12-, or 15-HPETE), which can be further reduced by glutathione peroxidase to the hydroxy forms (5-, 8-, 12-, 15-HETE), respectively [5–9]. The 5-LOX represents a dioxygenase that possesses two distinct enzymatic activities leading to the formation of LTA<sub>4</sub>. First, it catalyzes the incorporation of molecular oxygen into arachidonic acid (oxygenase activity), producing HPETE and subsequently forms the unstable epoxide LTA<sub>4</sub> by LTA<sub>4</sub> synthase activity [5,10]. This is followed by the insertion of molecular oxygen at position C-5, converting LTA<sub>4</sub> to either 5(S)-hydroxy-6-trans-8,11,14-cis-eicosatetraenoic acid (5-HETE) or leukotrienes. Thromboxane is a member of the family of lipids known as eicosanoids. It is produced in platelets by thromboxane-A synthase from the endoperoxides produced by the cyclooxygenase enzyme from arachidonic acid. Thromboxane synthase, a cytochrome P450 enzyme, catalyzes the conversion of the prostaglandin endoperoxide into thromboxane A<sub>2</sub> (TXA<sub>2</sub>), a potent vasoconstrictor and inducer of platelet aggregation. In concert with prostacyclin, TXA<sub>2</sub> plays a pivotal role in the maintenance of homeostasis. TXA<sub>2</sub> is a major oxygenated metabolite of arachidonic acid in the platelets [11]. TXA<sub>2</sub>, produced by activated platelets, has prothrombotic properties, stimulating activation of new platelets as well as increasing platelet aggregation. Platelet aggregation is achieved by mediating expression of the glycoprotein complex GPIIb/IIIa in the cell membrane of platelets. Circulating fibrinogen binds these receptors on adjacent platelets, further strengthening the clot. Prostacyclin is a member of the family of lipid molecules known as eicosanoids. These are produced in endothelial cells from PGH<sub>2</sub> by the action of the enzyme prostacyclin synthase. Although prostacyclin is considered as an independent mediator, it is called prostaglandin I<sub>2</sub> (PGI<sub>2</sub>) in eicosanoid nomenclature, and is a member of the prostanooids (together with the prostaglandins and thromboxane). PGI<sub>2</sub> is derived from the  $\omega$ -6 arachidonic acid. The series-3 prostaglandin PGH<sub>3</sub> also follows the prostacyclin synthase pathway, yielding another prostacyclin, PGI<sub>3</sub> [12]. PGI<sub>3</sub> is derived from the  $\omega$ -3 EPA. Prostacyclin acts as a vasodilator and prevent platelet formation and clumping involved in blood clotting. In the present study we address the mode of interaction of diaryl furan derivatives with the cyclooxygenase-2, thromboxane synthase, lipoxygenase and prostacyclin synthase active sites making use of docking to predict their binding affinities.

## 2. Materials and methods

### 2.1. Phylogenetic analysis

Reference protein of COX-2 from human (P35354) of well-established molecular function, was chosen as query sequence to search against human GenBank database, High Throughput

Genomic Sequences (HTG) and Non-Redundant (NR) using TBLASTN tool of National Center for Biotechnology Information (NCBI) [13]. A cutoff *E*-value (*e*-10) was previously set as selection criteria of BLAST hits for genomic sequences. The genomic sequences found were used to predict putative genes contained within them. The genes were predicted using GeneScan [14], GenomeScan [14], FGENESH [15], GeneMark (<http://opal.biology.gatech.edu/GeneMark/eukhmm.cgi>) and GrailEXP [16]. The sequences that have similar expression were found by BLAST searches against EST and NR databases of GenBank, using the genomic sequence as query. Each new predicted CDS served as a query sequence for new BLAST searches, leading to the identification of the largest possible number of related sequences. The predicted CDS were translated into amino acids and compared to the reference sequence. The protein sequences were aligned using ClustalW 1.8 [17]. Further, the multiple alignments were edited with the help of GENEDOC (Free Software Foundation, Inc.). Proteins with greater than 30% identity to that of the reference protein were regarded as functionally similar (homologous) to the reference protein and received the same name [18–21]. Those sequences that did not conform to this criterion were discarded. In each family, similar sequences were removed and the sequences were subjected to PROSITE and Pfam databases to see the presence of signature sequences for the corresponding families. The selected proteins were evaluated for the presence of transmembrane domains, using the HMMTOP algorithm [22]. Protein alignments obtained with ClustalW 1.8 [17] were used as starting points for phylogenetic analysis, based on the Parsimony method using TREEVIEW software [23]. In all cases, 1000 bootstrap replications tested the tree topology obtained.

### 2.2. Homology modelling

The sequence of human lipoxygenase (1–701 amino acids), thromboxane synthase (31–533 amino acids), and cyclooxygenase-2 (1–604 amino acids) enzymes (accession numbers: AAC79680.1, P24557, P35354) were obtained from NCBI and SWISSPROT. The 3D models of human lipoxygenase, thromboxane synthase, and cyclooxygenase-2 were built by using MODELLER 7v7 software on windows operating system [24]. Twenty models were generated for each of the protein structure used in this study. Template structures from the related family were predicted using BLAST server [13] against Protein Data Bank (PDB). Reference structures were chosen based on the sequence alignment that showed maximum identity with high score and less *e*-value to build 3D models for lipoxygenase, thromboxane synthase, and COX-2. The coordinates for the structurally conserved regions (SCRs) for query sequences were assigned from the template using pairwise sequence alignment, based on the Needleman–Wunsch algorithm [25,17].

### 2.3. Molecular dynamics studies

The structure with least modeller objective function obtained from the MODELLER was improved by molecular dynamics and equilibration methods using NAMD 2.5 software [26] and CHARMM22 force field for lipids and proteins [27–29] along with the TIP3P model for water [30]. The simulations began with a 10,000-step minimization of the designed side chains and solvent to remove any bad contacts. A cutoff of 12 Å (switching function starting at 10 Å) for van der Waals interactions was assumed. An integration time step of 2 fs was used, permitting a multiple time-stepping algorithm [31,32] to be employed, in which interactions involving covalent bonds were computed every time step. Short-range non-bonded interactions were computed every two-time step, and long-range electrostatic forces were computed every

four-time steps. The pair list of the non-bonded interaction was recalculated every 10 time steps with a pair list distance of 13.5 Å. The short-range non-bonded interactions were defined as van der Waals and electrostatics interactions between particles within 12 Å. A smoothing function was employed for the van der Waals interactions at a distance of 10 Å. The backbone atoms were harmonically constrained with a restraining constant of 10.0 kcal/mol Å<sup>2</sup>, and the systems were heated to 300 K over the course of 6 ps at constant volume. The simulations were equilibrated for 2 ns with NPT ensemble (1 atm, 300 K) while the harmonic constraints were gradually turned off. With no harmonic constraints, the simulations ran for 2 ns in the NPT ensemble using Langevin dynamics at a temperature of 300 K with a damping coefficient of  $\gamma = 5 \text{ ps}^{-1}$  [33]. Pressure was maintained at 1 atm using the Langevin piston method with a piston period of 100 fs, a damping time constant of 50 fs, and a piston temperature of 300 K. Non-bonded interactions were smoothly switched off from 10 to 12 Å. The list of non-bonded interactions was truncated at 14 Å. Covalent bonds involving hydrogen were held rigid using the SHAKE algorithm, allowing a 2 fs time step. No periodic boundary conditions were included for the above studies. Atomic coordinates were saved every 1 ps for the trajectory analysis during the last 2 ns of MD simulation. CHARMM22 force field parameters were used in all simulations in this study. Finally, the graph was drawn by taking Root Mean Square Deviation (RMSD) on X-axis with time (ns) on Y-axis. Structure with least RMSD of C $\alpha$  trace in the trajectory generated was used for further studies.

#### 2.4. Validation of 3D models and active site identification

The final structure obtained was analyzed by Ramachandran's map using PROCHECK (Programs to Check the Stereo Chemical Quality of Protein Structures) [34], environment profile using verify-3D (Structure Evaluation Server) [35] and ERRAT graphs [36]. ERRAT assesses the distribution of different types of atoms with respect to one another in the protein model. The residue packing and atomic contact analysis was performed by Whatif program [37] to identify bad packing of side chain atoms or unusual residue contacts. The software WHATCHECK [38] was used to obtain the Z-score of Ramachandran's plot. These models were used for the identification of active site and for docking of the inhibitors with the enzymes. The active site was predicted using an alpha shape algorithm to determine potential active sites in 3D protein structures in MOE site finder [39,40]. Binding sites were defined by atoms within 5.0 Å of the ligand or alpha spheres and trimmed at the edges to define a contiguous binding site surface of ~300 Å<sup>2</sup> of surface area.

#### 2.5. Docking studies and bioactivity

The inhibitors 4-(2-phenyl-3-thienyl) benzene sulfonamide, 4-(2-phenyltetrahydrofuran-3-yl) benzene sulfonamide, 4-(2-phenyl-1H-pyrrol-3-yl) benzene sulfonamide, 4-(5-phenyl-1H-imidazol-4-yl) benzene sulfonamide, 4-(5-phenyl-1,3-oxazol-4-yl) benzene sulfonamide, 4-(5-phenyl-1,3-thiazol-4-yl) benzene sulfonamide analogs including all hydrogen atoms, were built and optimized with CHEMSKETCH software suite. The top 30 compounds selected based on structural diversity and high affinity scores predicted using OPENEYE software suite were used for further docking against the homology models of human COX-2, lipoyxygenase, thromboxane synthase and crystal structures of mouse COX-2 and human prostacyclin synthase. Extremely Fast Rigid Exhaustive Docking (FRED) version 2.1 was used for docking studies (Open Eye Scientific Software, Santa Fe, NM). FRED docking roughly consists of 2 steps: shape fitting and optimization. During shape fitting, the ligand was placed into a 0.5-Å resolution grid box

encompassing all active site atoms (including hydrogen's) using a smooth Gaussian potential [41]. A series of three optimization filters were then processed, which consists of (1) refining the position of hydroxyl hydrogen atoms of the ligand, (2) rigid body optimization, and (3) optimization of the ligand pose in the dihedral angle space. In the optimization step, 4 scoring functions are available: Gaussian shape scoring [41], chemscore [42] PLP [43] and screenscore [44]. The binding pocket was defined using the ligand-free protein structure and a box enclosing the binding site. This box was defined by extending the size of a ligand by 4 Å (add box parameter of FRED). One unique pose for each of the best-scored compounds was saved for the subsequent steps. The compounds used for docking was converted in 3D with OMEGA which has previously been shown to select a conformation similar to that of the X-ray input when using appropriate parameters [45] (a low-energy cutoff to discard high energy conformations, a low RMSD value below which two conformations are considered to be similar, and a maximum of 500–1000 output conformations) (Open Eye Scientific Software, Santa Fe, NM). The bioavailability of compounds was assessed using adsorption, distribution, metabolism, elimination (ADME) prediction methods. Compounds were also tested to the Lipinski's rule of five using molinspiration [46]. Briefly, this rule is based on the observation that most orally administered drugs have a molecular weight of 500 or less, a log *P* no higher than five, 5 or fewer hydrogen bond donor sites and 10 or fewer hydrogen bond acceptor sites (N and O atoms). The polar surface areas (PSA) were also calculated since it is another key property linked to drug absorption, including intestinal absorption, bioavailability, Caco-2 permeability and blood-brain barrier penetration. Thus, passively absorbed molecules with a PSA > 140 Å<sup>2</sup> are thought to have low oral bioavailability. Drug likeliness was also calculated using OSIRIS server, which is based on a list of about 5300 distinct substructure fragments created by 3300 traded drugs as well as 15,000 commercially available chemicals yielding a complete list of all available fragments with associated drug likeliness [47]. The drug score combines drug likeliness, *c log P*, log *S*, molecular weight and toxicity risks as a total value that may be used to judge the compound's overall potential to qualify for a drug.

### 3. Results

#### 3.1. Phylogenetic analysis

Genome wide analysis of human COX sequences showed 11 characterized genes of COX-1 and 4 of COX-2. Percent identity for all the sequences was calculated in each family with the corresponding query sequence using GENEDOC (Free software foundation Inc.) based on multiple sequence alignment (Fig. 1). Multiple sequence alignment of COX-1 and COX-2 shows that Arg120 is highly conserved. Our results show that these proteins contain 1 transmembrane domain. Phylogenetic analysis of COX sequences revealed that COX-1 and COX-2 are divergent, showing branches in tree view (Fig. 2). It revealed two major families with five subfamilies of COX-1 indicating different functions to each family (Table 1).

#### 3.2. Homology modelling and validation

Reference proteins 1LOX, 1TQN and 3PGH have 26%, 32%, and 60% sequence identity with lipoyxygenase (1–701 amino acids), thromboxane synthase (31–533 amino acids) and COX-2 (19–570 amino acids) from human. These reference proteins were used as templates for modelling human lipoyxygenase, thromboxane synthase, and COX-2. Coordinates of structurally conserved regions (SCRs), structurally variable regions (SVRs), N-termini



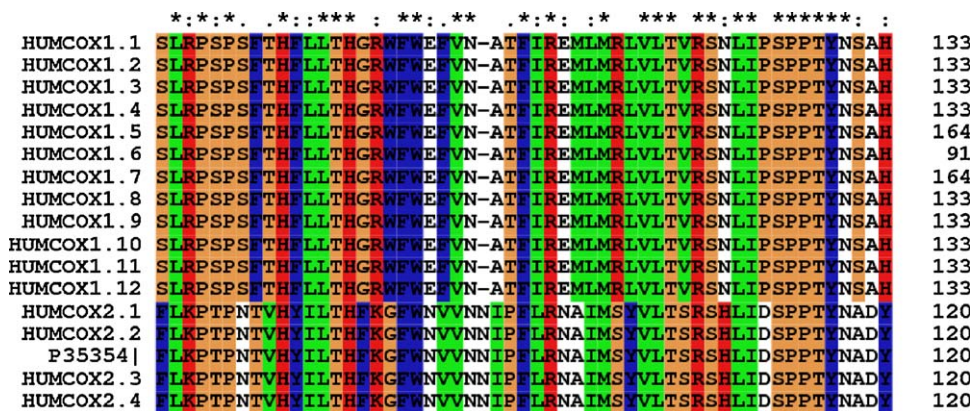


Fig. 1. Multiple sequence alignment of COX-1 and COX-2 predicted using clustalX software. Conserved residues are indicated with \*. Hum represents human.

and C-termini from the templates were assigned to the target sequences based on the satisfaction of spatial restraints. All side chains of the model protein were set by rotamers. The models generated were refined by molecular dynamics and equilibration method using NAMD software and the trajectory graph was drawn between the RMSD of C $\alpha$  trace on X-axis and time (ns) on Y-axis (Fig. 3). It was found from these figures that the RMSD was stable around 1.5 ns and then increased and decreased at 2 ns in case of human COX-2 (Fig. 3A) and it was stable for thromboxane synthase (Fig. 3B) and lipoyxygenase (Fig. 3C). Final stable structures of these three human proteins (prostacyclin synthase, thromboxane

synthase and human COX-2) contain 21, 21 and 27  $\alpha$ -helices, 18, 10 and 17  $\beta$ -sheets, respectively, as shown in Fig. 4. It appears from the Ramachandran's plot that 75.9%, 78.8% and 84.5% of the residues are located within the most favored, 20.8%, 18.7% and 13.9% in additionally allowed, 1.7%, 1.1% and 0.6% in generously allowed and 1.7%, 1.4% and 1.1% in disallowed regions for lipoyxygenase, thromboxane synthase, and COX-2, respectively. The RMSD for covalent bonds were  $-0.87$ ,  $-0.62$ ,  $-0.52$  and covalent angles were  $-12.63$ ,  $-1.99$ ,  $-1.94$  Å relative to the standard dictionary of human lipoyxygenase, thromboxane synthase and COX-2. Altogether 98.3% 98.6% and 98.9% of the residues of human lipoyxygenase, thromboxane synthase and COX-2 were in favored and allowed regions. The PROCHECK G-factor of human lipoyxygenase, thromboxane synthase and COX-2 was  $-5.58$ ,  $-1.15$  and  $-1.07$ . The overall quality factors of 70.425 for lipoyxygenase, 86.441 for thromboxane synthase and 93.360 for COX-2 were observed with the use of ERRAT environment profile. Also, 91.32% residues for COX-2 (Fig. 5A), 84.76% for thromboxane synthase (Fig. 5B) and 89.72% for lipoyxygenase (Fig. 5C) had an average 3D–1D score greater than 2 when verify-3D was used indicating that the models built are highly reliable. Evaluation of the final models of human lipoyxygenase, thromboxane synthase and COX-2 with Whatif program predicted the RMS Z-scores of backbone–backbone contacts which were  $-3.11$ ,  $-2.58$  and  $-1.52$ ; backbone–side chain contacts  $-2.01$ ,  $-1.87$  and  $-0.22$ ; side chain–backbone contacts  $-4.25$ ,  $-3.75$  and  $-2.62$  and side chain–side chain contacts  $-1.75$ ,  $-0.87$  and  $-0.99$ . Moreover, evaluation of the structural integrity of the final models of the above three human proteins showed Z-scores of  $-3.35$ ,  $-2.64$  and  $-1.56$ , which are closer to the normal value of 2.0 except for lipoyxygenase. This trend continued with the data obtained with the WHATCHECK program in which the Z-scores of bond lengths, bond angles, omega angle restraints, side chain planarity, improper dihedral distribution inside/outside distribution are 7.611, 2.915, 1.895, 3.005, 3.825 and 1.096 for the human lipoyxygenase; 1.633, 1.986, 1.785, 3.283, 1.866 and 1.057 for thromboxane synthase; 1.604, 2.007, 1.709, 3.226, 1.839 and 1.101 for COX-2, respectively. These values are positive indicating better conformation of the protein (positive is better than average) and are similar to those of the crystallographic structures.

### 3.3. Active site analysis

Possible binding sites of COX-2, thromboxane synthase, and human lipoyxygenase enzymes were searched using MOE software. The residues in lipoyxygenase 'Val8-Asp13', 'Leu15-Ser16', 'Phe41-Asp44', 'Lys79-Trp82', Arg95, Ile96, His98, 'Ile188-Leu196', Leu198, Leu205, Lys206, 'Ala397-Leu399', 'Glu401-Leu404', 'Ala406-Glu407',

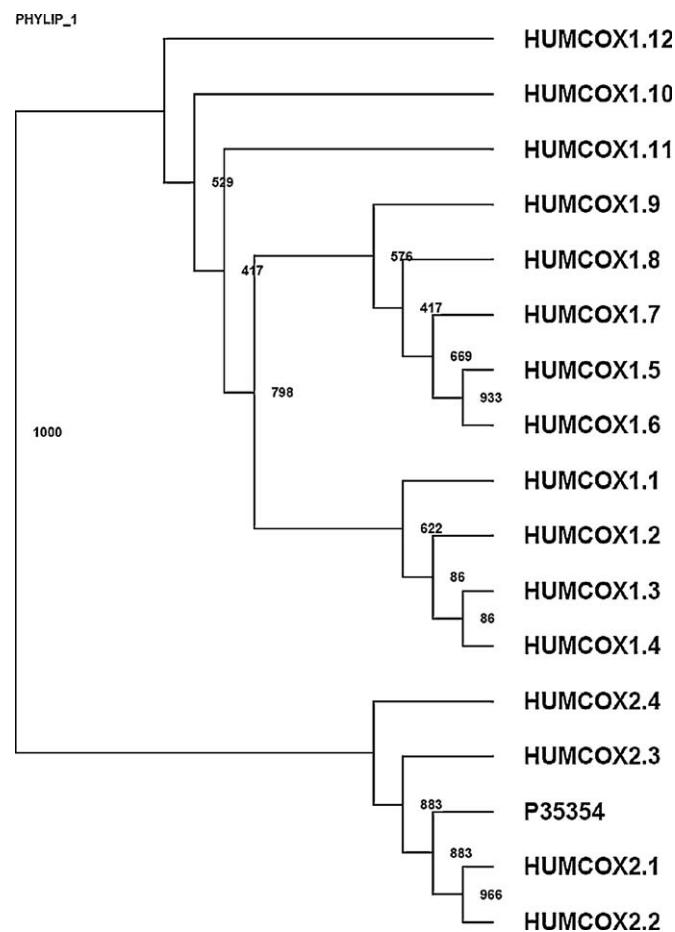


Fig. 2. Phylogenetic analysis of COX-1 and COX-2 sequences predicted using TREEVIEW software suite.

**Table 1**

BAC/PAC clone accession number, Genbank accession number, locus tag of the sequences, number of transmembrane segments, % identity with the query, gene name, full length cDNA sequences and EST accession numbers of both COX-1 and COX-2 genes predicted using various databases and software.

Sequence name	BAC/PAC clone accession number	GenBank accession number	Locus - tag	Number of TM segments	% Identity with Gene query name	Full length cDNA	ESTs accession number
HUMCOX1.1	S78220	AAB21215.1		1	58%		
HUMCOX1.2	AY449688	AAR08907.1		1	58%		
HUMCOX1.3	S36271	AAB22217.1		1	58%		
HUMCOX1.4	DQ895652	ABM86578.1		1	58% PTGS1		
HUMCOX1.5	DQ180742	ABA60099.1		1	55%		
HUMCOX1.6	AL162424	CAI14716.1	RP11-542K23.6-003	1	12%		
HUMCOX1.7	DQ180741	ABA60098.1			55%		
HUMCOX1.8	NM_000962	NP_000953.2		1	58%		
HUMCOX1.9	AL162424	CAI14715.1	RP11-542K23.6-001	1	58%		
HUMCOX1.10	AL162424	CAI14714.1	RP11-542K23.6-002	1	55%		
HUMCOX1.11	NM_080591	NP_542158.1		1	55%		
HUMCOX1.12	S36219	AAB22216.1		1	55%		
HUMCOX2.1	AJ634912	CAG25548.1			25%		
HUMCOX2.2	AY151286	AAN52932.1			53%		
HUMCOX2.3	AL033533	CAB41240.1	RP5-973M2.1-001		100% PTGS2	Em:AY151286.1	Em:AL710848.1 Em:BF939218.1 Em:BM129013.1 Em:BQ002136.1
						Em:AY462100.1	Em:CA436148.1
						Em:BC013734.1	Em:CA445948.1
						Em:L15326.1	Em:CB146285.1 Em:CB960307.1
						Em: M64291.1	Em:CD609928.1
						Em: M90100.1	Em:CD609929.1
						Em: U97696.1	Em:CD609930.1
HUMCOX2.4	NM_000963	NP_000954.1		1	100%		

'Asn594-Ala597', Met599, Arg600, 'Ile604-Thr606', Asn697 (Fig. 6A); in thromboxane synthase, 'Phe59-Phe63', Phe87, 'Asn109-Phe117', 'Ser119-Val120', 'Leu125-Phe126', Arg128, 'Asp177-Arg180', 'Thr182-Cys183', 'Lys214-Arg223', 'Ile225-Leu226', Leu229, Ile235, Leu239, 'Lys246-Asn247', Leu251, 'Phe336-Ile337', 'Ile340-Ala341', Tyr343, 'Glu344-Ile345', 'Thr347-Asn348', 'Ser351-Phe352', 'Pro406-Thr411', Glu413, Val430, Phe472, 'Arg477-Cys479', Val482, Leu512, 'Leu514-Gly521', Lys523, Gly525 and Val526 (Fig. 6B) and in human COX-2, 'His24-Gln30', 'Arg46-Phe49', Asn53, Glu58, Leu60, Thr61,

Lys64, Leu65, 'Lys68-Asn72', Val74, Leu78, Met99, 'Tyr101-Val102', Ser105, Arg106, 'His108-Leu109', Leu138, Val335, Leu338, Tyr341, Leu345, Glu451, 'Lys454-Pro460', 'Val509-Glu510', Ala513 and Leu517 (Fig. 6C) are highly conserved with the active site of templates. Residues 1–17 and 570–604 were removed from the model (human COX-2) because no homologous region occurred in 3PGH and these residues were not found near the active site. Therefore, the present model is made up of residues 18–569.

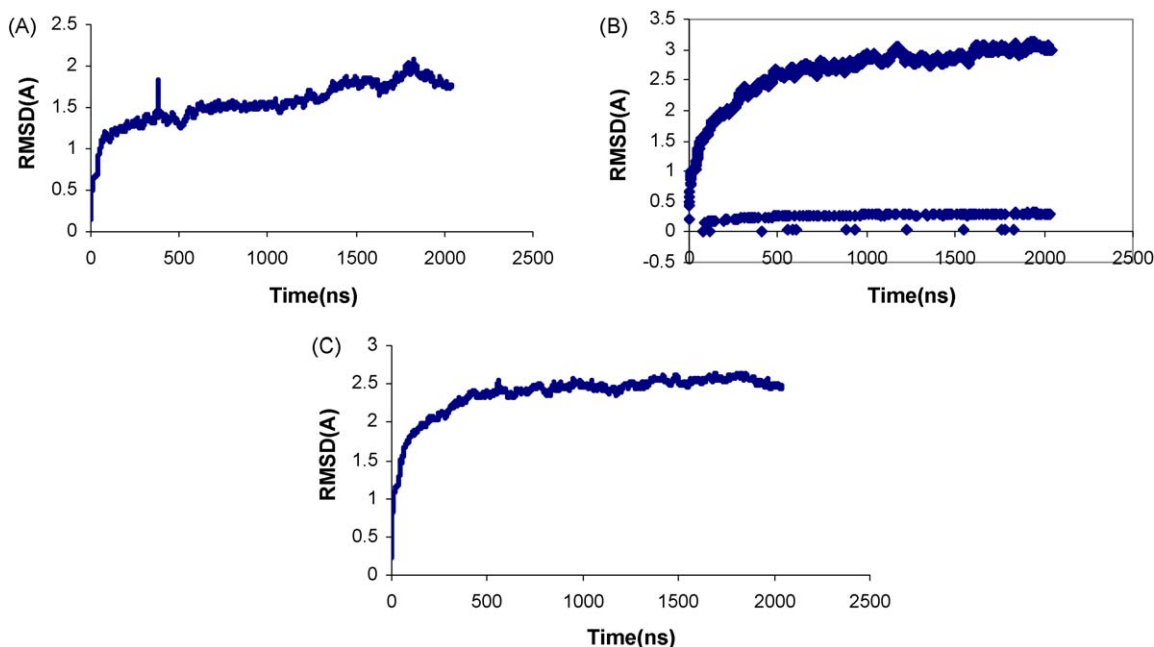


**Fig. 3.** Calculated RMSD graphs of molecular dynamics simulations of human cyclooxygenase-2 (A), thromboxane synthase (B) and lipoxygenase (C) using NAMD software. Time (ns) is taken on X-axis and RMSD (Å) on Y-axis.



**Fig. 4.** The created 3D structures of human cyclooxygenase-2 (A), thromboxane synthase (B) and lipoxigenase (C). The structure is obtained by energy minimization and equilibration over the last 1,00,000 runs with 2 ns of molecular dynamics simulation. The  $\alpha$ -helices is represented in ribbons and  $\beta$ -sheets is represented in yellow arrows. The pictures were taken from pymol software.

#### 3.4. Superimposition and secondary structure prediction

The RMSD of C $\alpha$  trace of final refined models of human COX-2 (Fig. 7A) thromboxane synthase (Fig. 7B) and lipoxigenase (Fig. 7C), and enzymes with the templates 1LOX, 1TQN and 3PGH was 1.68, 1.64 and 1.51 Å. The RMSD of C $\alpha$  trace of models generated from the MODELLER with the templates was 0.83, 0.30 and 0.17 Å with a difference of 1.38, 1.34 and 1.33 Å between initial and final refined models. These differences create conformational changes in the active site of enzymes. Secondary structures were also analyzed based on the superimposition of their 3D structures by SPDBV software suite (<http://www.expasy.org/spdbv>). The secondary structures of human COX-2 with that of template, was highly conserved with 25  $\alpha$ -helices and 14  $\beta$ -sheets with a difference of 2  $\alpha$ -helices at  $\alpha$ 1 and  $\alpha$ 9 and 2  $\beta$ -sheets at  $\beta$ 6 and  $\beta$ 16 (Fig. 8A). Also it was found that  $\alpha$ 2,  $\alpha$ 3,  $\alpha$ 4,  $\alpha$ 5,  $\alpha$ 7,  $\alpha$ 8,  $\alpha$ 13,  $\alpha$ 14,  $\alpha$ 19,  $\alpha$ 27,  $\beta$ 13, and  $\beta$ 14 are longer than the template. The secondary structures of human thromboxane synthase with that of template, was less conserved with 21  $\alpha$ -helices and 10  $\beta$ -sheets with a difference of 3  $\alpha$ -helices at  $\alpha$ 4,  $\alpha$ 11, and  $\alpha$ 13 and 2  $\beta$ -sheets at  $\beta$ 8 and  $\beta$ 9 (Fig. 8B). It was found that  $\alpha$ 5,  $\alpha$ 15,  $\alpha$ 17,  $\alpha$ 19,  $\alpha$ 20, and  $\alpha$ 21 are longer than the template. The secondary structures of human lipoxigenase with that of template were less conserved with 21  $\alpha$ -helices and 18  $\beta$ -sheets with a difference of 2  $\alpha$ -helices at  $\alpha$ 2 and  $\alpha$ 3, and 2  $\beta$ -sheets at  $\beta$ 4,  $\beta$ 9, and  $\beta$ 18 (Fig. 8C). It was

also found that  $\alpha$ 1,  $\alpha$ 4,  $\alpha$ 12,  $\alpha$ 14,  $\alpha$ 20, and  $\alpha$ 23 are longer than the template. In spite of several amino acid differences between the primary sequences of the model built with the template, their secondary structures are identical indicating that these models are reliable for docking.

#### 3.5. Docking studies of new diaryl furan derivatives

Calculated docking scores for the celecoxib derivatives designed by substituting different chemical groups on one of the benzene rings replacing 1H pyrazole group in celecoxib with different five member rings like thiophene, furan, 1H pyrrole, 1H imidazole, thiazole and 1,3-oxazole showed that most of the diaryl furan molecules showed good binding affinity towards mouse COX-2 (Table 2). The top 30 molecules showed high affinity scores with the crystal structure of COX-2 from mouse (PDB: 3PGH). Total docking scores of top 30 docked conformations of newly designed molecules with different side chains are shown in Table 3. It appears from this table that these inhibitors exhibit greater selectivity to thromboxane synthase and COX-2 compared to lipoxigenase and prostacyclin synthase. Molecules 2–5 are likely to have better thromboxane synthase selectivity with –1045.42, –1061.653 and –1077.886 scores compared to other enzymes. Molecule 5, which interacts with high affinity with thromboxane synthase, shows hydrogen-bonding interaction with main chain



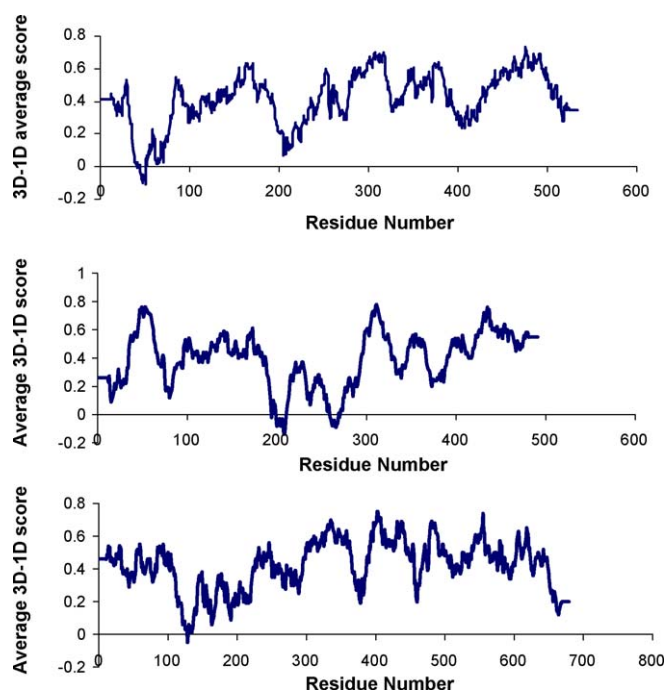


**Fig. 5.** The 3D profiles of human cyclooxygenase-2 (A), and thromboxane synthase (B) and lipoxigenase (C) models that were verified using verify-3D server. Overall compatibility score above zero indicates residues are reasonably folded.

oxygen of Met81. Molecules 1 and 5 interact with Arg120 and Phe518 of mouse COX-2 with two hydrogen-bonding interactions, where the sulfonamide group orients towards the Arg120 at the base of the active site, and the carboxylate group interacts with Phe518. In human COX-2, carboxylate group of molecule 2 interacts with the side chain atoms of Arg106 and Try341, a key catalytic residue just below the heme similar to Arg120 and Tyr355 as found in the crystal structure of mouse COX-2. This suggests that a compound with a CH<sub>2</sub>F group orients in the vicinity of Tyr341, such as molecule 5 and showed stronger inhibitory activity on thromboxane synthase than the compounds without CH<sub>2</sub>F group. Molecule 6 interacts with two hydrogen-bonding interactions with main chain oxygen atom of Tyr355 and O $\epsilon$  atom of Glu524, which in turn interact with Arg120 in the closed form exclusively. In the open conformation, Glu524 bridges between Arg120 and Arg513. Molecules 7–12 with CF<sub>3</sub> in the R<sup>2</sup> show better selectivity to thromboxane synthase than other enzymes. Inhibitor 7 that has a pyridyl ring in the R<sup>1</sup> position allows this part of the inhibitor to penetrate deep into hydrophobic pocket and shows greater binding affinity with thromboxane synthase compared to other enzymes by interacting with main chain oxygen of Arg379. Molecule 9 with 4-NO<sub>2</sub> in the R<sup>1</sup> position shows better binding affinity with human thromboxane synthase (–1126.585), compared to crystal structure of mouse COX-2 (–632.4), lipoxigenase (–322.23) and prostacyclin synthase (–439.44). This may provide additional hydrophobic and hydrophilic interactions. The nitro groups are close to the charged residue Arg120 lying at the entrance of the COX-2 active site. The phenyl group fills the top of the channel and is stabilized by  $\pi$ – $\pi$  interactions with Trp387 and Phe518, respectively. CH– $\pi$  interaction is also observed between Tyr355 and the phenyl rings. Molecule 9, the best of the series of inhibitors with a high affinity of –1126.585 with thromboxane synthase shows two hydrogen-bonding interactions with main chain oxygen of Met81 and Ser83, compared to COX-2 from mouse and human lipoxigenase and prostacyclin synthase. Molecules 16 and 18 show almost equal affinity with thromboxane synthase, human and mouse COX-2. With CHF<sub>2</sub> in the R<sup>2</sup> position, the

binding affinity varies from 18 to 21 and shows high affinity (–866.857) against thromboxane synthase compared to M19 (–850.624), M20 (–866.857), M21 (–883.09) but least activity with prostacyclin synthase (Table 3). Hydrogen-bonding interaction shows that 21, 25, 27 and 29 bind with NH<sub>2</sub> group of Arg106 in COX-2, oxygen of Met81, O $\gamma$  of Ser83, O $\epsilon$ 1 of Glu188, NZ of Lys216, NH of Arg80 and main chain oxygen of Met81 in thromboxane synthase enzyme. Molecule 29 interacts with fluoride and CO<sub>2</sub>Me in the R<sup>1</sup> and R<sup>2</sup> positions and shows high binding affinity with thromboxane synthase by binding with NH atom of Arg80 and main chain oxygen of Met81 with –1012.954 compared to other enzymes. It is interesting to note that molecule 6 with OMe group (in place of CF<sub>3</sub>) seems to retain thromboxane synthase and COX-2 preference over lipoxigenase and prostacyclin synthase. These studies show that binding scores of all the compounds are better for thromboxane synthase and COX-2 than lipoxigenase and prostacyclin synthase. Therefore, these molecules elevate the levels of prostacyclin synthase that inhibits thrombosis for the people undergoing myocardial infraction. Site directed mutagenesis of Arg120Ala, Ser530Ala, Ser530Met and Tyr355Phe of mouse COX-2 abolishes the activity of molecules 4–6 and reduces the activity of other molecules compared to wild type. This indicates that these are the important determinant residues for the activity of COX-2 (Table 4). To evaluate the results of docking accuracy, known inhibitors (pyroxicam, nimesulide, naproxen, mefenamic acid, meclofenamic acid, ketoralac, indomethacin, ibuprofen and diclofenac) were docked against wild and mutant types of mouse COX-2 (PDB: 3PGH). Pyroxicam shows two hydrogen-bonding interactions with NH<sub>1</sub> and OH groups of Arg120 and Tyr355 (Fig. 9A), nimesulide shows five hydrophobic interactions with C $\gamma$ 1, C $\gamma$ , C $\delta$ 1, C $\epsilon$ 2 and C $\gamma$ 2 atoms of Val349, Leu352, Leu359, Phe518 and Val523 (Fig. 9B), naproxen shows two hydrogen-bonding with NH<sub>1</sub> and OH groups of Arg120 and Tyr355 and five hydrophobic interactions with C $\gamma$ 1, C $\delta$ 2, C $\delta$ 1, C $\epsilon$ 2 and C $\gamma$ 1 atoms of Val349, Leu352, Leu359, Phe518 and Val523 (Fig. 9C), mefenamic acid shows two hydrogen-bonding interaction with OH and O $\gamma$  atoms of Tyr385 and Ser530 and eight hydrophobic interactions with C $\gamma$ 1, C $\delta$ 2, C $\epsilon$ 1, C $\delta$ 1, C $\epsilon$ 2, C $\gamma$ , C $\gamma$ 1 and C $\gamma$  atoms of Val349, Leu352, Phe381, Leu384, Trp387, Met522, Val523 and Leu531 (Fig. 9D), meclofenamic acid shows single hydrogen-bonding with O $\gamma$  atom of Ser119 and seven hydrophobic interactions with C $\gamma$ 1, C $\delta$ 1, CH<sub>2</sub>, C $\gamma$ 2, C $\beta$ , C $\delta$ 2 and C $\delta$ 2 atoms of Val89, Leu39, Trp100, Ile112, Val116, Phe357 and Leu359 (Fig. 9E), ketoralac shows seven hydrophobic interactions with C $\gamma$ 1, C $\delta$ 2, C $\epsilon$ 1, C $\delta$ 1, C $\epsilon$ 2, C $\gamma$  atoms of Val349, Leu352, Phe381, Leu384, Trp387, Met522 and Leu531 (Fig. 9F), indomethacin shows C $\delta$ 1, C $\gamma$ 2, C $\gamma$ , C $\delta$ 2, C $\gamma$ 2 and C $\gamma$  atoms of Leu93, Val116, Val349, Leu384, Trp387, Phe518, Met522 and Val523 residues, respectively (Fig. 9G), ibuprofen shows two hydrogen-bonding interactions with NH<sub>1</sub> and OH groups of Arg120 and Tyr355 and eight hydrophobic interactions with C $\gamma$ 2, C $\gamma$ 1, C $\delta$ 2, C $\delta$ 1, C $\epsilon$ 2, C $\gamma$ , C $\gamma$ 2 and C $\delta$ 1 atoms of Val116, Val349, Leu352, Leu359, Trp387, Met522, Val523 and Leu531 (Fig. 9H) and diclofenac shows one hydrogen-bonding interaction with Tyr385 and eight hydrophobic interactions with C $\gamma$ 2, C $\gamma$ , C $\epsilon$ 1, C $\delta$ 1, C $\epsilon$ 2, C $\gamma$  and C $\gamma$ 1 atoms of Val349, Leu352, Phe381, Leu384, Trp387, Phe518, Met522 and Val523 residues, respectively (Fig. 8I). Total docking scores calculated are shown in Table 5 and it is clear from the table that the aryl carboxylic acid, meclofenamic acid are equipotent against wild type enzyme (–585.39) and Ser530Ala (–585.39) but exhibit reduced inhibition of the Tyr355Phe with a docking score of –569.3. Inhibition by indomethacin was very sensitive to mutation of Arg120Ala, Tyr355Phe and Ser530Ala with the docking scores of –712.18, –748.95 and –717.75. Studies on mutagenesis and with the crystal structure of COX-2 indomethacin complex shows that, carboxylic acid of indomethacin interacts with Arg120 and Tyr355 with the

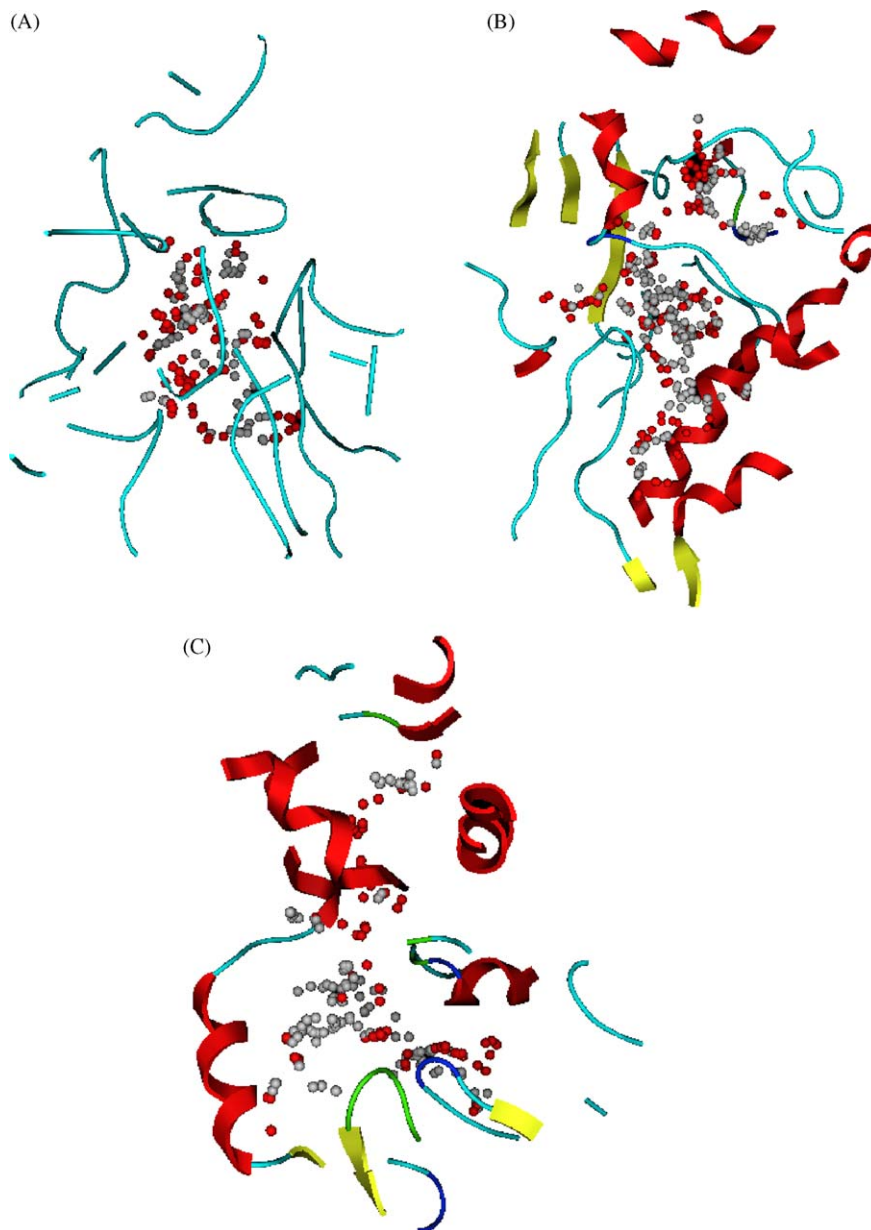


**Fig. 6.** Active site of lipoxigenase (A), thromboxane synthase (B) and cyclooxygenase-2 (C) predicted using MOE software.  $\alpha$ -helices are represented in red color,  $\beta$ -sheets is represented in green and loops are represented in magenta. Active site area is represented in spheres.

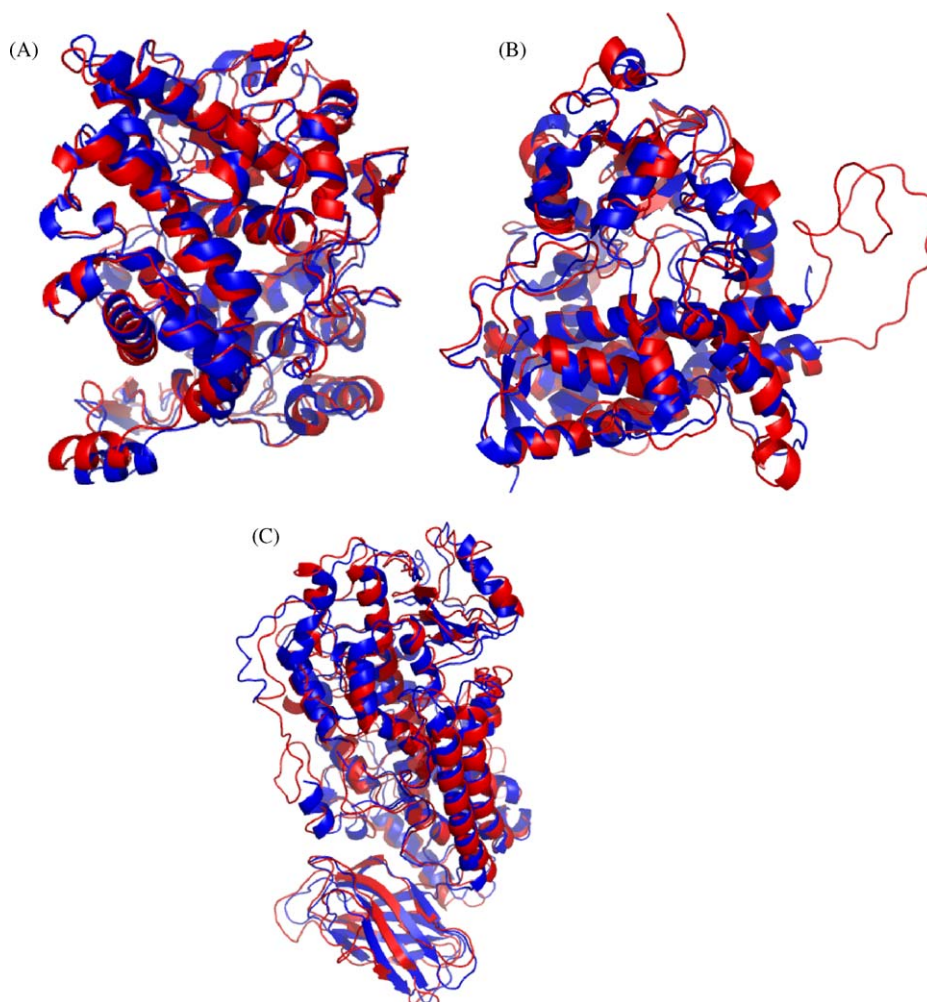
bond distances of 2.4 and 3.0 Å, respectively [48–51]. Ser530Ala enzymes are completely resistant to inhibition by diclofenac (–573.22) and show no significant effect on Arg120Ala and Tyr355Phe based on the docking scores for wild (–535.97) and mutant types (–561.04, and –577.97). However, arylcarboxylic acid, ketorolac did not inhibit Arg120Ala or Ser530Ala with the docking scores of –565.39 and –577.75 but showed inhibitory activity against Tyr355Phe with docking scores of –592.71. Pyroxicam contains no carboxylic acid, but showed inhibitory activity against Tyr355Phe with docking score of –744.96 compared to wild type that displayed –735.64. Nimesulide showed no impact on Arg120Ala, Tyr355Phe and Ser530Ala. Our studies also show that nimesulide has weaker inhibition activity against Ser530Ala. Thus, mutation of Ser530Ala suggests that it binds to COX-2 to maximize interaction with the Ser530 hydroxyl group. Naproxen shows impact on the inhibition of Tyr355Phe enzyme with docking score of –551.93 compared to wild type score of –617.8 (Table 5). Mefenamic acid exhibits no impact on Arg120Ala, Tyr355Phe and Ser530Ala. Ibuprofen displays reduced

activity against Tyr355Phe with the docking scores of –472.67 but no activity on Arg120Ala and Ser530Ala with docking scores of –488.73 and –483.87. A regression analysis of docking scores and  $\log I_{C_{50}}$  for NSAIDs was carried out and the scatter plots are drawn for wild and mutant types as shown in Fig. 10. It was found that the  $r^2$  values for wild type (Fig. 10A), Arg120Ala (Fig. 10B), Tyr355Phe (Fig. 10C) and Ser530Ala (Fig. 10D) mutants are 0.81, 0.96, 0.63 and 0.59, respectively. These graphs show that docking scores correlate well with the results obtained from experimental data [52]. Hence, docking results of these inhibitors perhaps can be used as a new pharmacophore for lead generation and optimization of novel antithrombotic and anti-inflammatory agents. On the basis of docking results and bioavailability scores (Table 6), compound 4 is predicted to be the best antithrombotic and anti-inflammatory.

#### 4. Discussion

To design efficient inhibitors against the crystal structure of COX-2, phylogenetic analysis of all the COX-2 sequences was

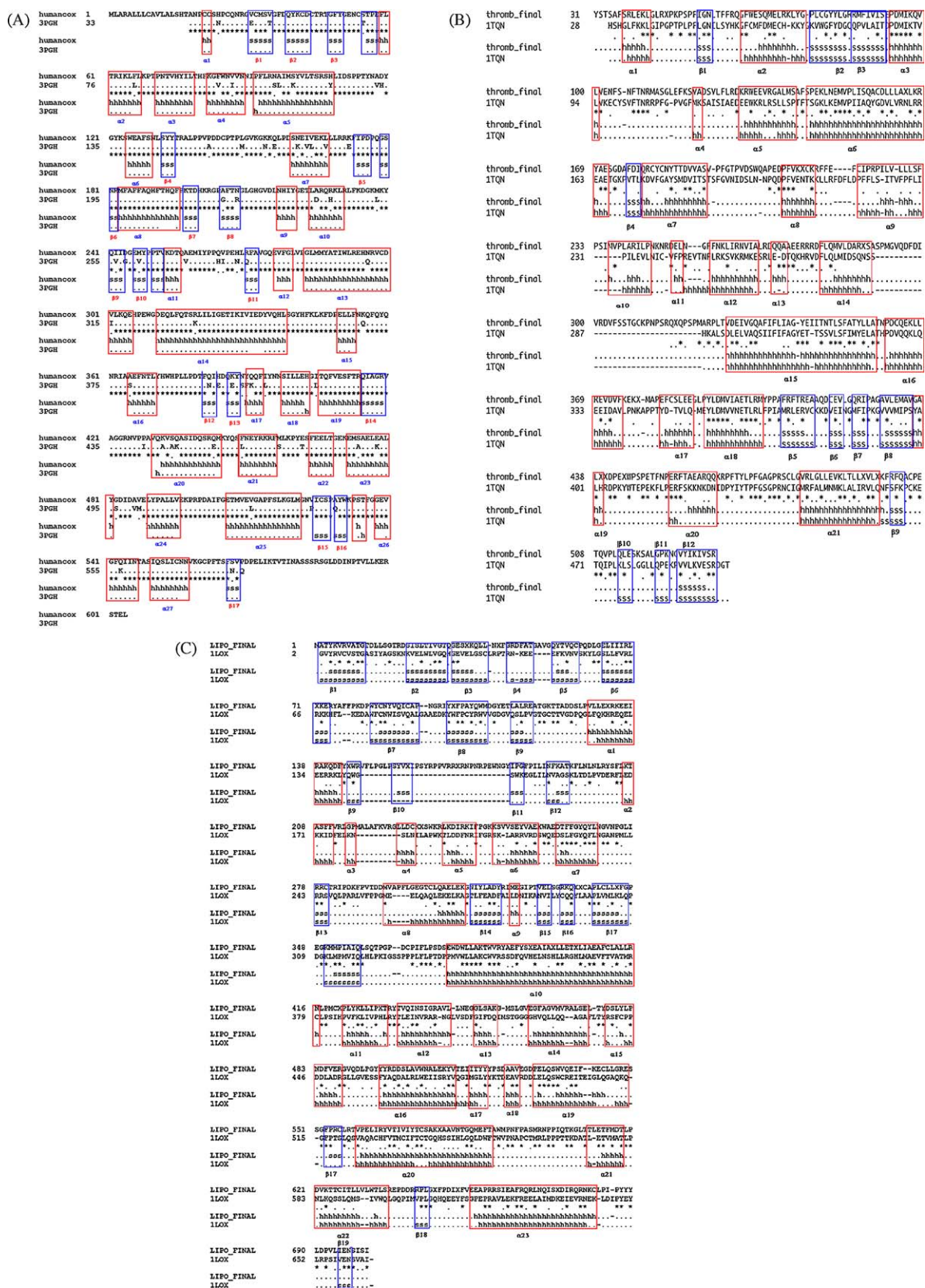




**Fig. 7.** Superimposition of C $\alpha$  trace of cyclooxygenase-2 (A), thromboxane synthase (B) human lipoxygenase (C) (represented in red) and the templates 1PXX, 1TQN and 1LOX (represented in blue color).

carried out using the entire human genome. Phylogenetic analysis revealed 11 COX-1 and 4 COX-2 sequences. It appeared that both COX-1 and COX-2 sequences are highly conserved in their secondary structures and in the active site of the protein except for the residue Val523 in COX-2 by Ile in COX-1 [46]. Identity of both COX-1 and COX-2 sequences were above 55% but HUMCOX1.6 and HUMCOX2.3 showed less than 30% identity with reference sequence. Phylogenetic tree also revealed that the COX-1 sequences form five sub-families. HUMCOX1.1–1.4 are closely related to one another and form one sub-family, HUMCOX1.5–1.9 form into another but HUMCOX2.0–2.2 forms separate branches in the phylogenetic tree. Also it was noticed that only HUMCOX2.3 in COX-2 contains ESTs and cDNA libraries. Based on these findings, it appears that both COX-1 and COX-2 sequences are related to one another in the evolution with high percentage of identity and similarity. A homology model for human COX-2, thromboxane synthase and lipoxygenase was derived based on the pairwise sequence alignment using 3PGH, 1TQN and 1LOX as the templates. Interestingly, the average pairwise RMS fit of the C- $\alpha$  coordinates of these homologs was very less, indicating a strong structural conservation. Refinement of the homology model resulted in a structure with a least RMSD compared to the unrefined structure. The Ramachandran plot showed that more than 98% of residues were occupying the allowed region and no key or important residues are seen in the disallowed regions. Verify-3D analysis suggested that  $\beta$ -3 in human COX-2, loop between  $\alpha$ 7 and  $\alpha$ 8 in

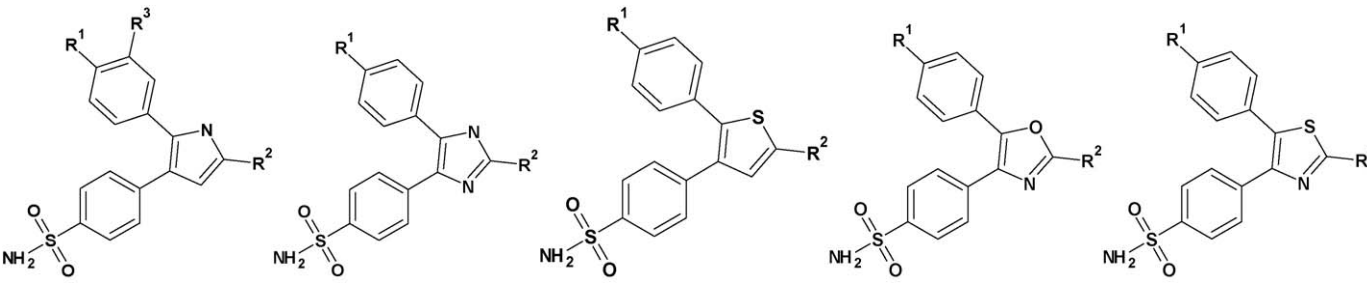
thromboxane synthase and  $\alpha$ 1 of lipoxygenase were slightly misfolded and does not appear in the active sites of any of the 3D structures. In summary, the above-mentioned analyses indicate that the model structures are consistent with current understanding of protein structure. Docking studies with 4-(2-phenyl-3-thienyl) benzene sulfonamide, 4-(2-phenyltetrahydrofuran-3-yl) benzene sulfonamide, 4-(2-phenyl-1H-pyrrol-3-yl) benzene sulfonamide, 4-(5-phenyl-1H-imidazol-4-yl) benzene sulfonamide, 4-(5-phenyl-1,3-oxazol-4-yl) benzene sulfonamide, 4-(5-phenyl-1,3-thiazol-4-yl) benzene sulfonamide analogs against mouse crystal structure show that diaryl furan derivatives bind effectively than the other molecules used in the study. Docking studies with 4-(2-phenyltetrahydrofuran-3-yl) benzene sulfonamide analogs against human lipoxygenase, thromboxane synthase and COX-2 revealed that they bind effectively with stronger hydrogen-bonding interactions. It appears that His90, Arg120, Gln192, Leu352, Tyr355, Tyr385, Phe470, Phe518, Glu524, Gly526, Ser530 of mouse COX-2, Arg106 and Tyr341 of human COX-2 are the main residues involved in hydrogen-bonding interactions. These studies also reveal that when central ring oxygen interacts with Arg120, sulfonamide moves into the side pocket of the active site and is involved in hydrogen bonds with polar residues such as His90 and Arg513 and also hydrogen bonded to Glu524. These interactions are essential for COX-2 inhibitory activity as exemplified by the binding interactions of SC558, an analog of celecoxib, co-crystallized in COX-2 active site [48]. The side chains occupy a nonpolar

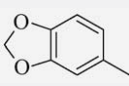


**Fig. 8.** Secondary structure alignment of human cyclooxygenase-2 (A), thromboxane synthase (B) and lipoxigenase (C) with the template 1PXX, ITQN and 1LOX were predicted using SPDBV software suite. α-Helices is represented in red color boxes and β-sheets is represented in blue color boxes.

**Table 2**

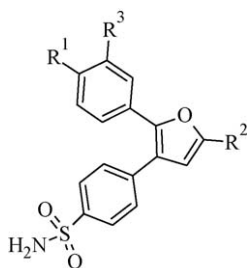
Total docking scores of top 30 molecules of docked conformations of newly designed inhibitors based on 1H pyrrole, 1H imidazole, thiophene, 1,3-oxazole, 1,3-thiazole group against crystal structure of mouse cyclooxygenase-2 (PDB: 3PGH), predicted using OPENEYE software. Total score is sum of chemguass score, chemscore, PLP score, screenscore and shapeguass score.



Comp	R <sup>1</sup>	R <sup>2</sup>	R <sup>3</sup>	1H pyrrole	1H imidazole	Thiophene	Furan	1,3-Oxazole	1,3-Thiazole
1	F	CO <sub>2</sub> H		-496.29	-479.18	-527.1	-711.86	-547.63	-520.74
4	Cl	CH <sub>2</sub> OH		-753.16	-692.36	-415.78	-646.1	-528.91	-520.38
5	H	CH <sub>2</sub> F		-768.27	-704.9	-410.72	-643.36	-527.87	-520.36
6	H	OMe		-783.38	-717.44	-405.66	-640.62	-526.83	-520.34
7	2-Pyridyl	CF <sub>3</sub>		-798.49	-729.98	-400.6	-637.88	-525.79	-520.32
8	4-Pyridyl	CF <sub>3</sub>		-813.6	-742.52	-395.54	-635.14	-524.75	-520.3
9	4-NO <sub>2</sub>	CF <sub>3</sub>		-828.71	-755.06	-390.48	-632.4	-523.71	-520.28
10	4-NH <sub>2</sub>	CF <sub>3</sub>		-511.4	-491.72	-522.04	-706.38	-546.59	-520.72
11	4-NHMe	CF <sub>3</sub>		-526.51	-504.26	-516.98	-703.64	-545.55	-520.7
12	4-CH <sub>2</sub> OH	CF <sub>3</sub>		-541.62	-516.8	-511.92	-700.9	-544.51	-520.68
14	F	H		-556.73	-529.34	-501.8	-695.42	-543.47	-520.66
19	4-CONH <sub>2</sub>	CHF <sub>2</sub>		-571.84	-541.88	-476.5	-678.98	-542.43	-520.64
20	4-CO <sub>2</sub> H	CHF <sub>2</sub>		-586.95	-554.42	-466.38	-676.24	-540.35	-520.6
21	4-OMe	CHF <sub>2</sub>		-602.06	-566.96	-461.32	-673.5	-539.31	-520.58
22	3-Fluoro-4-methoxy	CHF <sub>2</sub>	-617.17	-579.5	-456.26	-670.76	-538.27	-520.56	
23	5-Methyl-2-furyl	CHF <sub>2</sub>		-632.28	-592.04	-451.2	-668.02	-537.23	-520.54
24		CHF <sub>2</sub>		-647.39	-604.58	-446.14	-665.28	-536.19	-520.52
25	H	CHF <sub>2</sub>		-662.5	-617.12		-662.54	-535.15	-520.5
26	F	CO <sub>2</sub> Me		-677.61	-629.66	-441.08	-659.8	-534.11	-520.48
27	H	CH <sub>3</sub>		-692.72	-642.2	-436.02	-657.06	-533.07	-520.46
28	Cl	CH <sub>2</sub> OH		-707.83	-654.74	-430.96	-654.32	-532.03	-520.44
29	H	CH <sub>2</sub> F		-722.94	-667.28	-425.9	-651.58	-530.99	-520.42

**Table 3**

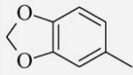
Docking scores of top 30 molecules of docked conformations of newly designed inhibitors based on furan group against crystal structure of mouse cyclooxygenase-2 (PDB: 3PGH), homology models of human cyclooxygenase-2, lipoxigenase and thromboxane synthase, predicted using OPENEYE software. Total score is sum of chemguass score, chemscore, PLP score, screenscore and shapeguass score.



Comp	R <sup>1</sup>	R <sup>2</sup>	R <sup>3</sup>	3PGH	Human COX-2	Thromboxane synthase	Lipoxygenase	Prostacyclin synthase
1	F	CO <sub>2</sub> H		-711.86	-619.24	-652.56	-599.25	-705.68
4	Cl	CH <sub>2</sub> OH		-646.1	124.14	-1045.42	-373.53	-
5	H	CH <sub>2</sub> F		-643.36	157.93	-1061.653	-363.27	-480.4
6	H	OMe		-640.62	191.72	-1077.886	-353.01	-470.16
7	2-Pyridyl	CF <sub>3</sub>		-637.88	225.51	-1094.119	-342.75	-459.92
8	4-Pyridyl	CF <sub>3</sub>		-635.14	259.3	-1110.352	-332.49	-449.68
9	4-NO <sub>2</sub>	CF <sub>3</sub>		-632.4	293.09	-1126.585	-322.23	-439.44
10	4-NH <sub>2</sub>	CF <sub>3</sub>		-706.38	-585.45	-680.74	-588.99	-695.44
11	4-NHMe	CF <sub>3</sub>		-703.64	-551.66	-706.67	-578.73	-685.2
12	4-CH <sub>2</sub> OH	CF <sub>3</sub>		-700.9	-517.87	-720.76	-568.47	-674.96

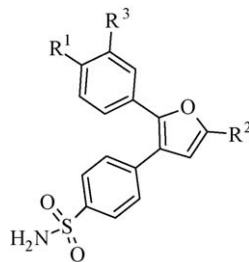


**Table 3** (Continued)

Comp	R <sup>1</sup>	R <sup>2</sup>	R <sup>3</sup>	3PGH	Human COX-2	Thromboxane synthase	Lipoxygenase	Prostacyclin synthase
13	CONH <sub>2</sub>	Cl	Cl	−698.16	−484.08	−736.993	−558.21	−664.72
14	F	H		−695.42	−450.29	−753.226	−547.95	−654.48
15	H	F	H	−692.68	−416.5	−769.459	−537.69	−644.24
16	H	SO <sub>2</sub> Me	Cl	−689.94	−382.71	−785.692	−527.43	−634
17	H	NH <sub>2</sub>	H	−687.2	−348.92	−818.158	−517.17	−623.76
18	4-SO <sub>2</sub> Me	CHF <sub>2</sub>		−681.72	−315.13	−834.391	−506.91	−613.52
19	4-CONH <sub>2</sub>	CHF <sub>2</sub>		−678.98	−281.34	−850.624	−496.65	−603.28
20	4-CO <sub>2</sub> H	CHF <sub>2</sub>		−676.24	−247.55	−866.857	−486.39	−593.04
21	4-OMe	CHF <sub>2</sub>		−673.5	−213.76	−883.09	−476.13	−582.8
22	3-Fluoro-4-methoxy	3-Fluoro-4-methoxy	CHF <sub>2</sub>	−670.76	−179.97	−899.323	−465.87	−572.56
23	5-Methyl-2-furyl	CHF <sub>2</sub>		−668.02	−146.18	−915.556	−455.61	−562.32
24		CHF <sub>2</sub>		−665.28	−112.39	−931.789	−445.35	−552.08
25	H	CHF <sub>2</sub>		−662.54	−78.6	−948.022	−435.09	−541.84
26	F	CO <sub>2</sub> Me		−659.8	−44.81	−964.255	−424.83	−531.6
27	H	CH <sub>3</sub>		−657.06	−11.02	−980.488	−414.57	−521.36
28	Cl	CH <sub>2</sub> OH		−654.32	22.77	−996.721	−404.31	−511.12
29	H	CH <sub>2</sub> F		−651.58	56.56	−1012.954	−394.05	−500.88

**Table 4**

Total docking scores of top 30 molecules of docked conformations of newly designed inhibitors based on furan group against mutants of mouse cyclooxygenase-2 (PDB: 3PGH), predicted using OPENEYE software. Total score is sum of chemguass score, chemscore, PLP score, screen score and shapeguass score.



Comp	R <sup>1</sup>	R <sup>2</sup>	R <sup>3</sup>	Arg120Ala	Ser530Ala	Ser530Met	Tyr355Phe
1	F	CO <sub>2</sub> H		−453.08	−454.85	−454.85	−454.85
4	Cl	CH <sub>2</sub> OH		74.94	158.47	93.91	158.47
5	H	CH <sub>2</sub> F		106	190.75	126.19	190.75
6	H	OMe		137.06	223.03	158.47	223.03
7	2-Pyridyl	CF <sub>3</sub>		168.12	255.31	190.75	255.31
8	4-Pyridyl	CF <sub>3</sub>		199.18	287.59	223.03	287.59
9	4-NO <sub>2</sub>	CF <sub>3</sub>		230.24	319.87	255.31	319.87
10	4-NH <sub>2</sub>	CF <sub>3</sub>		−422.02	−390.29	−422.57	−390.29
11	4-NHMe	CF <sub>3</sub>		−390.96	−358.01	−390.29	−358.01
12	4-CH <sub>2</sub> OH	CF <sub>3</sub>		−359.9	−1203.15	−358.01	−325.73
13	CONH <sub>2</sub>	Cl	Cl	−328.84	−293.45	−325.73	−293.45
14	F	H		−297.78	−261.17	−293.45	−261.17
15	H	F	H	−266.72	−554.62	−261.17	−228.89
16	H	SO <sub>2</sub> Me	Cl	−235.66	−196.61	−228.89	−196.61
17	H	NH <sub>2</sub>	H	−204.6	−164.33	−196.61	−164.33
18	4-SO <sub>2</sub> Me	CHF <sub>2</sub>		−173.54	−99.77	−164.33	−99.77
19	4-CONH <sub>2</sub>	CHF <sub>2</sub>		−142.48	−67.49	−132.05	−67.49
21	4-OMe	CHF <sub>2</sub>		−111.42	−35.21	−99.77	−35.21
23	5-Methyl-2-furyl	CHF <sub>2</sub>		−80.36	−2.93	−67.49	−2.93
26	F	CO <sub>2</sub> Me		−49.3	29.35	−35.21	29.35
28	Cl	CH <sub>2</sub> OH		−18.24	61.63	−2.93	61.63
29	H	CH <sub>2</sub> F		12.82	93.91	29.35	93.91

cleft in the entry channel and are bounded by Val116, Met113, Ile112, Phe357, Leu369 and Leu93. The inhibitors assume their final binding position in which the side chains occupy the central channel. Known inhibitors diclofenac, pyroxicam and nimesulide showed no inhibition against site directed mutagenesis of Ser530Ala enzyme but diclofenac exhibits effect on Arg120Ala, Tyr355Phe and Ser530Met enzymes. Diclofenac also showed activity against Arg120Ala and Ser530Met mutants of COX-2

[51,53]. Llorens et al. suggested two conformations of diclofenac bound to COX-2 in which the dichlorophenyl group projects down into the main channel of the active site [55]. Our docking scores suggest that Ser530Ala and Ser530Met are inhibited by pyroxicam. This indicates that Arg120, Tyr355 and Ser530 are involved in interactions in extended conformations. Mutation in any one of these residues abolishes inhibition activity. It can be predicted therefore that these residues are important for binding in the COX

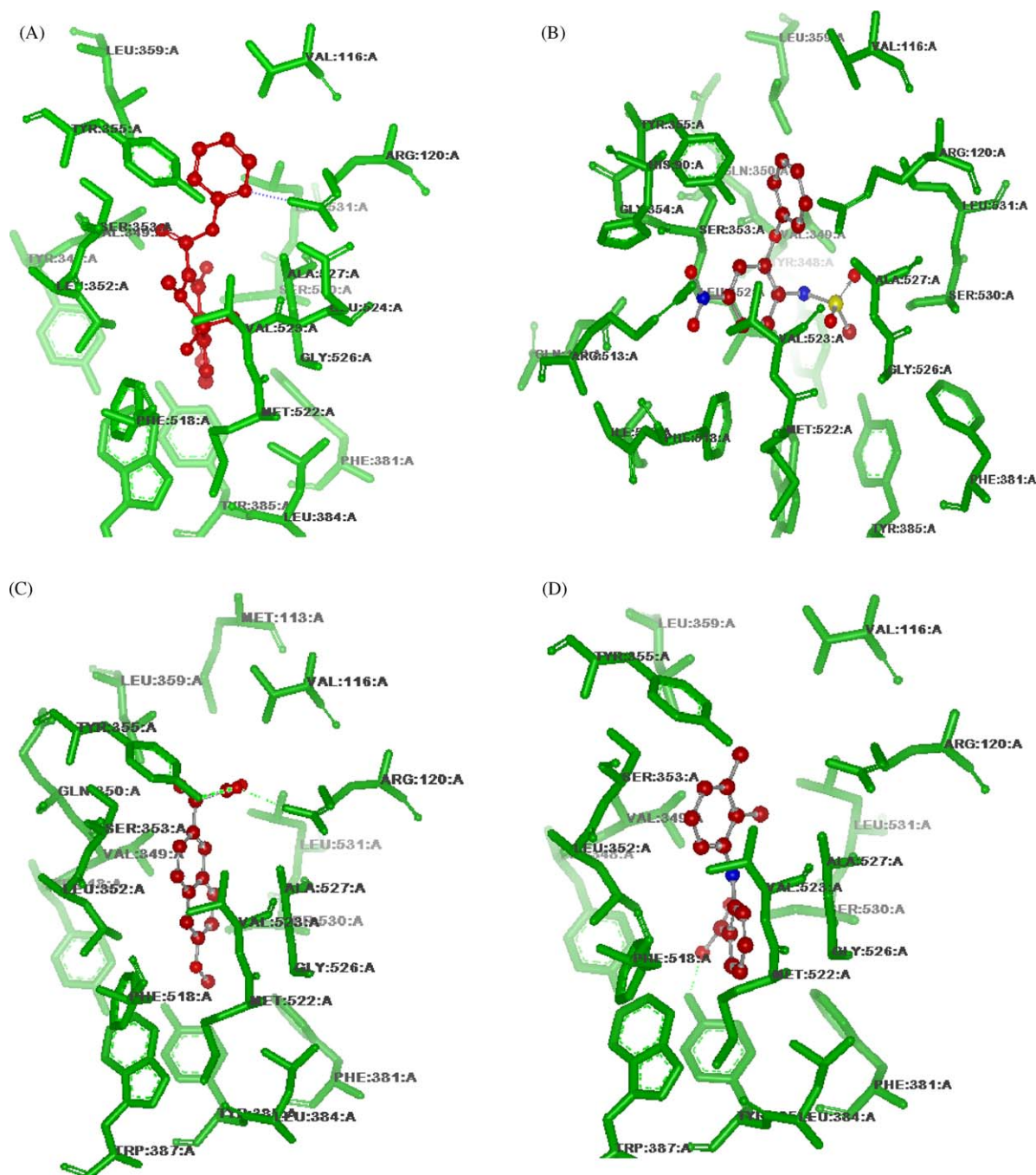
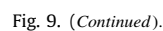


**Fig. 9.** Binding of pyroxicam (A), nimesulide (B), naproxen (C), mefenamic acid (D), meclofenamic acid (E), ketorolac (F), indomethacin (G) and ibuprofen (H) and diclofenac (I) in the active site of mouse cyclooxygenase-2 enzyme (PDB: 3PGH). Ligands are represented in ball and stick model and residues are labeled in black colors. Protein is represented in green color.

active site. Further, mutation of Ser530Ala and Ser530Met inhibits the activity suggesting that polar nitro group of Ser530 is involved in hydrogen bond interaction with nimesulide. Our studies show that these molecules bind to COX-2 in an extended conformation involving interaction with all the residues. A suitable position of the two polar groups near Arg120 and in the hydrophilic side pocket seems to be important. Moreover, involvement of the phenyl ring in  $\pi$ – $\pi$  interactions at the top of the channel probably leads to an enhanced COX-2 activity. Our studies and also existing literature demonstrate that three distinct anchoring sites contribute to substrate and inhibitor binding in the COX active site. The first anchoring site lies at the junction of Arg120 and Tyr355 near membrane surface. These residues drive the affinity and

orientation of inhibitors. The second major anchoring point is the side pocket, defined by residues Tyr355, Val523, His90, Gln192 and Arg513. The selectivity of diaryl heterocyclic inhibitors that contain phenylsulfonamides is in part determined by interactions in this side pocket. Similarities in the binding modes of these inhibitors support the possibility of substrate inhibition in COX-2. Mutation in any of the residues abolishes inhibitory activity suggesting that concerted interaction with all the three residues is perhaps essential for binding in the active site of COX-2. For example, these inhibitors do not efficiently inhibit the Tyr385Phe mutant of COX-2. This indicates that Tyr385 plays an important role in positioning the side chain and enhancing its chemical reactivity with Ser530. Mutation of Ser530 to methionine causes



Total docking scores of NSAIDS against wild and mutant types of cyclooxygenase-2 form mouse (PDB: 3PGH), predicted using OPENEYE software suite.

Ligand	Wild type	Arg120Ala	Tyr355Phe	Ser530Ala
Pyroxicam	−735.64	−697.97	−735.93	−732.95
Nimesulide	−552.94	−576.25	−584.91	−562.71
Naproxen	−617.8	−604.73	−551.13	−612.38
Mefenamic Acid	−632.24	−620.39	−621.03	−637.95
Meclofenamic Acid	−585.39	−557.23	−569.3	−585.39
Ketorolac	−589.29	−565.39	−592.71	−577.75
Indomethacin	−697.99	−712.18	−748.95	−717.75
Ibuprofen	−493.85	−488.73	−472.67	−483.87
Diclofenac	−535.97	−561.04	−560.7	−573.22



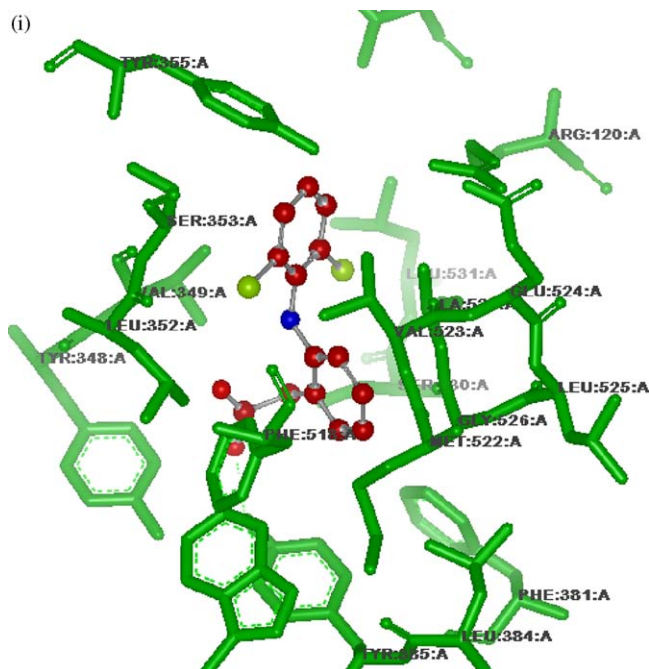
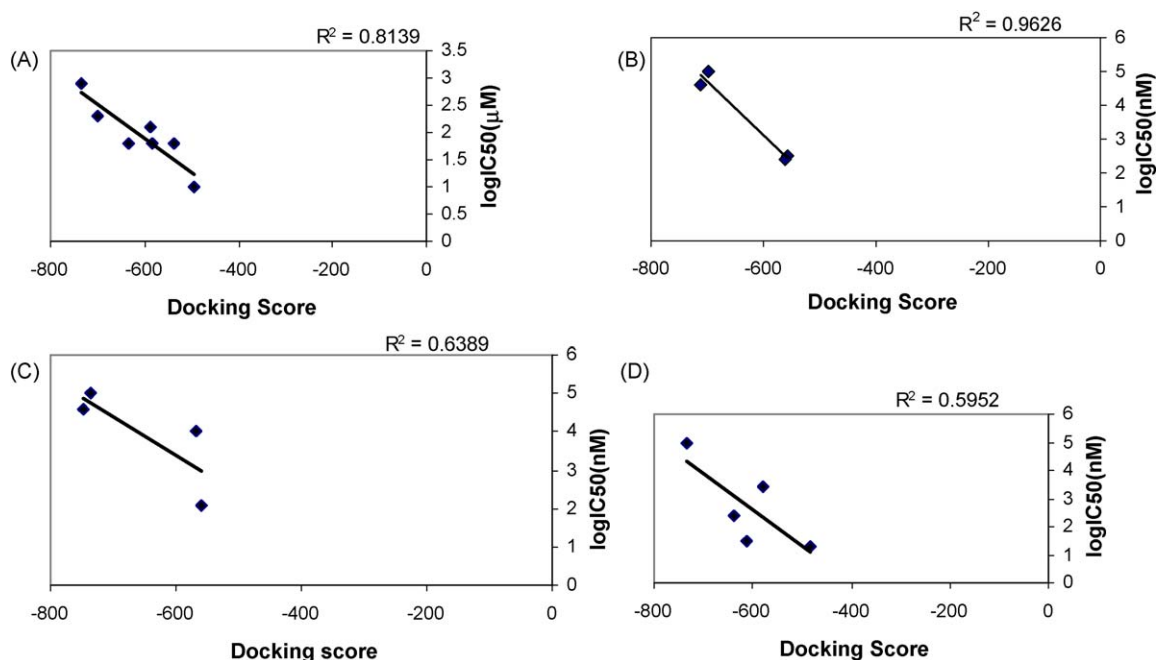


Fig. 9. (Continued).

increased bulkiness compared to acetylated serine, which results in a decreased interaction with the inhibitors in the active site. This also causes better interactions with the inhibitors due to nonpolar groups of methionine compared to mutation of Ser530 to alanine. Mancini et al. [54] showed the importance of Ser530 of COX-2 for interaction with fenamate inhibitors, diclofenac and meclofenamic acid. It appears that Arg110, Glu218, Arg223, Ser518, Ile221, Tyr343, Glu344, Asn348, Pro406, Ala407, Phe472, Ser478, Ala519 and Leu520 are important determinant residues involved in hydrogen-bonding interactions with thromboxane synthase. Docking studies with thromboxane synthase indicate that there

is sufficient space in the active site for simultaneous occupancy by diaryl furan derivatives in several possible combinations. Studies with lipoxygenase reveal that the sulfonamide group is oriented towards the entrance of the enzyme-binding site. The NH<sub>2</sub> group of sulfonamide moiety is located with hydrogen-bonding contact range of the amino acid residues Lys286, His336, Ser359, Asp365, Lys454, Ser478, Cys626, Thr634, Arg213 and Gly215. Docking studies with prostacyclin synthase show that inhibitors bind with Cδ1 of Phe96, Cβ of Leu103, NZ atom of Lys121, Nδ2 of Asn287, main chain nitrogen of Thr358, NH1 of Arg359, Nδ2 of Asn439 and main chain oxygen of Phe483 with less affinity. The side chain of Leu103 faces the substrate-binding channel and the hydrophilic residue Asn287 is nearer to heme involved in substrate binding as shown by Chiang et al. [55]. Docking scores and hydrogen-bonding interactions show that these molecules act as best inhibitors against thromboxane synthase, COX-2 and lipoxygenase and display least binding affinity to prostacyclin synthase. It is known that these molecules inhibit the levels of prostacyclin synthase in people undergoing myocardial infraction. Linear regression analysis between the docking scores and the experimental activities of known inhibitors showed a good correlation indicating that the docking scores are highly reliable. A model with the correlation coefficient ( $r^2$ ) of 0.62 was obtained for 8 compounds (diclofenac, ibuprofen, indomethacin, ketorolac, meclofenamic acid, mefenamic acid and pyroxicam) using the equation  $Y = -0.006x - 1.793$ . Removal of naproxen identified as outlier from the docking dataset yields a better model with correlation coefficient ( $r^2$ ) of 0.81. This good correlation demonstrates that the binding conformations and models of the known inhibitors with the crystal structure of mouse COX-2 are reasonable. Removal of ketorolac from the dataset yields an excellent model with the  $r^2$  of 0.96 and 0.63 in Arg120Ala and Tyr355Phe. Similarly, removal of diclofenac from the dataset yields a good model with the  $r^2$  of 0.59 in Ser530Ala mutants, respectively. Bioactivity of the molecules predicted using molinspiration server [46] shows (Table 5) five rotatable bonds with a molecular weight in between 300 and 500, log  $P$  value between 1 and 5, hydrogen bond donors between 2 and 6 and acceptors between 2 and 4 with zero violations. The drug



**Fig. 10.** Correlation of experimental affinities (IC<sub>50</sub>) and their docking scores against wild type (A), Arg120Ala (B), Tyr355Phe (C) and Ser530Ala (D) calculated using OPENEYE software.

**Table 6**

Biological activity values of top 30 2-cyclohexa-2,4-dien-1-yl-3-phenylfuran analogs calculated using molinspiration server. Drug likeliness and drug scores were calculated using OSIRIS server.

Mol	R <sup>1</sup>	R <sup>2</sup>	R <sup>3</sup>	Mi log P	TPSA	N atoms	MW	N ON	N OHNH	N rothb	Vol	Drug likeliness	Drug score
1	F	CO <sub>2</sub> H		3.2	110.6	25	361.3	6	3	4	283.0	0.36	0.49
4	Cl	CH <sub>2</sub> OH		1.2	93.5	24	362.8	5	3	4	286.4	2.03	0.54
6	H	OMe	H	0.7	82.5	23	328.3	5	2	4	274.1	1.2	0.52
13	CONH <sub>2</sub>	Cl	Cl	3.6	116.3	26	411.2	6	4	4	308.4	2.67	0.45
14	F	H		3.4	73.3	22	317.3	4	2	3	256.0	0.32	0.4
16	H	SO <sub>2</sub> Me	Cl	0.5	73.3	22	312.3	4	2	3	265.1	1.08	0.43
17	H	NH <sub>2</sub>	H	0.4	107.4	26	410.8	6	2	4	310.1	2.11	0.4
18	4-SO <sub>2</sub> Me	CHF <sub>2</sub>		2.7	99.3	22	314.3	5	4	3	262.4	1.11	0.48
27	H	CH <sub>3</sub>		0.7	73.3	22	312.3	4	2	3	265.1	1.08	0.53

likeliness of the molecules was predicted using the OSIRIS server [47], which is based on the comparison of the 5000-marketed drugs (positives) and 10,000 carefully selected non-drug compounds (negatives). It shows that molecules 1, 4, 6, 13, 14, 16, 17, 18 and 27 contain positive scores within the range of 0–2.6. These results indicate that the above-mentioned molecules act as drugs and inhibit the activity of COX-2 and thromboxane synthase enzymes. The results also show that molecule with chlorine and CH<sub>2</sub>OH in the R<sup>1</sup> and R<sup>2</sup> position binds with high affinity with thromboxane synthase and COX-2 but shows no affinity against prostacyclin synthase. This indicates that this molecule may be the best inhibitor for COX-2 and thromboxane synthase. These data indicate that 2-cyclohexa-2; 4-dien-1-yl-3-phenylfuran analogs inhibit the enzyme in lesser concentrations in the biological system and thus may help people undergoing myocardial infarction. Thus, it is hoped that these newly designed molecules if synthesized and tested in animal models hold promise for anti-inflammatory and antithrombosis activities.

## 5. Conclusions

The prostaglandin endoperoxide H synthases-1 and 2 (PGHS-1 and PGHS-2; also called COX-1 and COX-2) catalyze the committed step in prostaglandin synthesis. COX-1 and 2 are of particular interest because they are the major targets of non-steroidal anti-inflammatory drugs (NSAIDs) like aspirin, ibuprofen and the new COX-2 inhibitors. Inhibition of COX with NSAIDs acutely reduces inflammation, pain, and fever. But long-term use of these drugs reduces thrombotic events and increases the development of colon cancer and Alzheimer's disease. Our docking studies identified potential anti-inflammatory agents among the diaryl furan derivative class of compounds that act through a COX-2 and thromboxane synthase inhibition mechanism. The results indicate that 4-(2-phenyl-3-thienyl) benzene sulfonamide; 4-(2-phenyltetrahydrofuran-3-yl) benzene sulfonamide possesses significant anti-inflammatory and antithrombosis activity that are comparable to that of other inhibitors. Bioactivity of these inhibitors shows that these molecules inhibit the enzymes at very low concentrations. Thus, this study will be useful for the designing of novel anti-inflammatory and antithrombotic inhibitors.

## References

- [1] N.V. Chandrasekharan, H. Dai, K.L. Roos, N.K. Evanson, J. Tomsik, T.S. Elton, COX-3, a cyclooxygenase-1 variant inhibited by acetaminophen and other analgesic/antipyretic drugs: cloning, structure, and expression, *Proc. Natl. Acad. Sci. U.S.A.* 99 (2002) 13926–13931.
- [2] S. Narumiyama, Y. Sugimoto, F. Ushikubi, Ab initio gene finding in *Drosophila* genomic DNA, *Physiol. Rev.* 79 (1999) 1193–1226.
- [3] L.J. Marnett, Aspirin and the potential role of prostaglandins in colon cancer, *Cancer Res.* 52 (1992) 5575–5589.
- [4] C.J. Rieke, A.M. Mulichak, R.M. Garavito, W.L. Smith, The role of arginine 120 of human prostaglandin endoperoxide H synthase-2 in the interaction with fatty acid substrates and inhibitors, *J. Biol. Chem.* 274 (1999) 17109–17114.
- [5] C.D. Funk, Prostaglandins and leukotrienes: advances in eicosanoid biology, *Science* 294 (2001) 1871–1875.
- [6] L. Iversen, K. Kragballe, Prostaglandins Other Lipid Mediat. 63 (2000) 25–42.
- [7] S. Yamamoto, H. Suzuki, M. Nakamura, K. Ishimura, Arachidonate 12-lipoxygenase isozymes, *Adv. Exp. Med. Biol.* 447 (1999) 37–44.
- [8] A.R. Brash, M. Jisaka, W.E. Boeglin, M.S. Chang, Regulation of 15-lipoxygenase isozymes and mucin secretion by cytokines in cultured normal human bronchial epithelial cells, *Adv. Exp. Med. Biol.* 447 (1999) 29–36.
- [9] H. Kuhn, S. Borngraber, Mammalian 15-lipoxygenases. Enzymatic properties and biological implications, *Adv. Exp. Med. Biol.* 447 (1999) 5–28.
- [10] Y. Cao, S.M. Prescott, Many actions of cyclooxygenase-2 in cellular dynamics and in cancer, *J. Cell Physiol.* 190 (2002) 279–286.
- [11] B. Samuelsson, Prostaglandins and Thromboxanes, Academic Press, Inc., New York, 1977, pp. 133–154.
- [12] S. Fischer, P.C. Weber, Thromboxane (TX) A<sub>3</sub> and prostaglandin (PG) I<sub>2</sub> are formed in man after dietary eicosapentaenoic acid: identification and quantification by capillary gas chromatography–electron impact mass spectrometry, *Biomed. Mass Spectrom.* 12 (1985) 470–476.
- [13] S.F. Altschul, W. Gish, W. Miller, E.W. Myers, D.J. Lipman, Basic local alignment search tool, *J. Mol. Biol.* 215 (1990) 403–410.
- [14] C. Burge, S. Karlin, Prediction of complete gene structures in human genomic DNA, *J. Mol. Biol.* 268 (1997) 78–94.
- [15] A.A. Salamov, V.V. Solovyev, Ab initio gene finding in *Drosophila* genomic DNA, *Genome Res.* 10 (2000) 516–522.
- [16] Y. Xu, E.C. Uberbacher, Automated gene identification in large-scale genomic sequences, *J. Comput. Biol.* 4 (1997) 325–338.
- [17] J.D. Thompson, D.G. Higgins, T.J. Gibson, CLUSTAL W: improving the sensitivity of progressive multiple sequence alignment through sequence weighting, position-specific gap penalties and weight matrix choice, *Nucleic Acids Res.* 22 (1994) 4673–4680.
- [18] C.A. Orengo, D.T. Jones, J.M. Thornton, Protein domain superfolds and superfamilies, *Nature* 372 (1994) 631–634.
- [19] B. Rost, A. Valencia, Pitfalls of protein sequence analysis, *Curr. Opin. Biotechnol.* 7 (1996) 457–461.
- [20] B. Rost, Twilight zone of protein sequence alignments, *Protein Eng.* 12 (1999) 85–94.
- [21] A.E. Todd, C.A. Orengo, J.M. Thornton, Domain assignment for protein structures using a consensus approach: characterization and analysis, *J. Mol. Biol.* 307 (2001) 1113–1143.
- [22] T. Hirokawa, S. Boon-Chieng, S. Mitaku, SOSUI: classification and secondary structure prediction system for membrane proteins, *Bioinformatics* 14 (1998) 378–379.
- [23] R.D.M. Page, TreeView: an application to display phylogenetic trees on personal computers, *Comp. Appl. Biosci.* 12 (1996) 357–358.
- [24] A. Sali, T.L. Blundell, Comparative protein modelling by satisfaction of spatial restraints, *J. Mol. Biol.* 234 (1993) 779–815.
- [25] S.B. Needleman, C.D. Wunsch, A general method applicable to the search for similarities in the amino acid sequence of two proteins, *J. Mol. Biol.* 48 (1970) 443–453.
- [26] L. Kale, R. Skeel, M. Bhandarkar, R. Brunner, A. Gursoy, N. Krawetz, J. Phillips, A. Shinozaki, K. Varadarajan, K. Schulten, NAMD2: Greater scalability for parallel molecular dynamics, *J. Comput. Phys.* 151 (1999) 283–286.
- [27] A.D. MacKerell Jr., D. Bashford, M. Bellott, R.L. Dunbrack, J. Evanseck Jr., M.J. Field, S. Fischer, J. Gao, H. Guo, S. Ha, D. Joseph, L. Kuchnir, K. Kuczcera, F.T.K. Lau, C. Mattos, S. Michnick, T. Ngo, D.T. Nguyen, B. Prodhom, I.W.E. Reiher, B. Roux, M. Schlenkrich, J. Smith, R. Stote, J. Straub, M. Watanabe, J. Wiorcikiewicz-Kuczcera, D. Yin, M. Karplus, Self-consistent parameterization of biomolecules for molecular modeling and condensed phase simulations, *FASEB* 6 (1992) A143–A143.
- [28] A.D. MacKerell Jr., D. Bashford, M. Bellott, R.L. Dunbrack, J. Evanseck Jr., M.J. Field, S. Fischer, J. Gao, H. Guo, S. Ha, D. Joseph, L. Kuchnir, K. Kuczcera, F.T.K. Lau, C. Mattos, S. Michnick, T. Ngo, D.T. Nguyen, B. Prodhom, I.W.E. Reiher, B. Roux, M. Schlenkrich, J. Smith, R. Stote, J. Straub, M. Watanabe, J. Wiorcikiewicz-Kuczcera, D. Yin, M. Karplus, All-hydrogen empirical potential for molecular modeling and dynamics studies of proteins using the CHARMM22 force field, *J. Phys. Chem. B* 102 (1998) 3586–3616.
- [29] M.J. Schlenkrich, J. Brickmann, A.D. MacKerell Jr., M. Karplus, K.M. Merz, in: K.M. Merz, B. Roux (Eds.), *A Molecular Perspective from Computation and Experiment*, Birkhauser, Boston, MA, USA, 1996, pp. 31–81.

- [30] W.L. Jorgensen, J. Chandrasekhar, J.D. Madura, R.W. Impey, M.L. Klein, Comparison of simple potential functions for simulating liquid water, *J. Chem. Phys.* 79 (1983) 926–935.
- [31] H. Grubmüller, H. Heller, A. Windemuth, K. Schulten, Generalized, Verlet algorithm for efficient molecular dynamics simulations with long-range interactions, *Mol. Simulat.* 6 (1991) 121–142.
- [32] T.R. Schlick, A. Skeel, L. Brunger, J.A. Kale, J. Board Jr., K. Hermans, Schulten algorithmic challenges in computational molecular biophysics, *J. Comput. Phys.* 151 (1999) 9–48.
- [33] A. Brünger, X-PLOR Version 3.1: A System for X-Ray Crystallography and NMR, Yale University, New Haven, CT, USA, 1992.
- [34] R.A. Laskowski, M.W. MacArthur, D.S. Moss, J.M. Thornton, PROCHECK: a program to check the stereochemical quality of protein structures, *J. Appl. Cryst.* 26 (1993) 283–291.
- [35] R. Luthy, et al., Assessment of protein models with 3-dimensional profiles, *Nature* 356 (1992) 83–85.
- [36] Colovos, T.O. Yeates, Verification of protein structures: patterns of non-bonded atomic interactions, *Protein Sci.* 2 (1993) 1511–1519.
- [37] G. Vriend, WHAT IF: a molecular modeling and drug design program, *J. Mol. Graph.* 8 (1990) 52–56.
- [38] R.W.W. Hooft, G. Vriend, C. Sander, E.E. Abola, Errors in protein structures, *Nature* 381 (1996) 272–275.
- [39] H. Edelsbrunner, M. Facello, R. Fu, J. Liang, Measuring proteins and voids in proteins, *Science* (1995) 256–264.
- [40] J. Liang, H. Edelsbrunner, C. Woodward, Anatomy of protein pockets and cavities: measurement of binding site geometry and implications for ligand design, *Protein Sci.* 7 (1998) 1884–1897.
- [41] M.R. McGann, H.R. Almond, A. Nicholls, J.A. Grant, F.K. Brown, Gaussian docking functions, *Biopolymers* 68 (2003) 76–90.
- [42] M.D. Eldridge, C.W. Murray, T.R. Auton, G.V. Paolini, R.P. Mee, Empirical scoring functions: the development of a fast empirical scoring function to estimate the binding affinity of ligands in receptor complexes, *J. Comput. Aided Mol. Des.* 11 (1997) 425–445.
- [43] D.K. Gehlhaar, G.M. Verkhivker, P.A. Rejto, C.J. Sherman, D.B. Fogel, L.J. Fogel, S.T. Freer, Molecular recognition of the inhibitor AG-1343 by HIV-1 protease: conformational flexible docking by evolutionary programming, *Chem. Biol.* 2 (1995) 317–324.
- [44] M. Stahl, M. Rarey, Detailed analysis of scoring functions for virtual screening, *J. Med. Chem.* 44 (2001) 1035–1042.
- [45] J. Bostrom, J.R. Greenwood, J. Gottfries, Assessing the performance of OMEGA with respect to bioactive conformations, *J. Mol. Graph. Model.* 21 (2003) 449–462.
- [46] Molinspiration Cheminformatics, <http://www.molinspiration.com>.
- [47] [www.rndchemicals.com/drug-relevant-properties.html](http://www.rndchemicals.com/drug-relevant-properties.html).
- [48] R.G. Kurumbail, A.M. Stevens, J.K. Gierse, J.J. McDonald, R.A. Stegeman, J.Y. Pak, D. Gildehaus, J.M. Miyashiro, T.D. Penning, K. Seibert, P.C. Isakson, W.C. Stallings, Structure basis for selective inhibition of cyclooxygenase-2 by antiinflammatory agents, *Nature* 384 (1996) 644–648.
- [49] J.A. Mancini, D. Riendeau, J.P. Falgueyret, P.J. Vickers, G.P. O'Neill, Arginine 120 of prostaglandin G/H synthase-1 is required for the inhibition by nonsteroidal anti-inflammatory drugs containing a carboxylic acid moiety, *J. Biol. Chem.* 270 (1995) 29372–29377.
- [50] D.K. Bhattacharyya, M. Lecomte, C.J. Rieke, R.M. Garavito, W.L. Smith, Involvement of arginine 120, glutamate 524, and tyrosine 355 in the binding of arachidonate and 2-phenylpropionic acid inhibitors to the cyclooxygenase active site of ovine prostaglandin endoperoxide H synthase-1, *J. Biol. Chem.* 271 (1996) 2179–2184.
- [51] G.M. Greig, D.A. Francis, J.P. Falgueyret, M. Ouellet, M.D. Percival, P. Roy, C. Bayly, J.A. Mancini, G.P. O'Neill, The interaction of arginine 106 of human prostaglandin G/H synthase-2 with inhibitors is not a universal component of inhibition mediated by nonsteroidal anti-inflammatory drugs, *Mol. Pharmacol.* 52 (1997) 829–838.
- [52] S.W. Rowlinson, J.R. Kiefer, J.J. Prusakiewicz, L. Jennifer, K.R. Pawlitz, Kozak, S.K. Amit, C. William, S.G. Ravi, Kurumbail, L.J. Marnett, A novel mechanism of cyclooxygenase-2 inhibition involving interactions with Ser-530 and Tyr-385 14 (2003) 45763–45769.
- [53] O. Llorens, J.J. Perez, A. Palomer, D. Mauleon, Differential binding mode of diverse cyclooxygenase inhibitors, *J. Mol. Graph. Model.* 20 (2002) 359–371.
- [54] J.A. Mancini, P.J. Vickers, G.P. O'Neill, C. Boily, J.P. Falgueyret, D. Riendeau, Altered sensitivity of aspirin-acetylated prostaglandin G/H synthase-2 to inhibition by nonsteroidal anti-inflammatory drugs, *Mol. Pharmacol.* 51 (1997) 52–60.
- [55] C.W. Chiang, H.C. Yeh, L.H. Wang, N.L. Chan, Crystal structure of the human prostacyclin synthase, *J. Mol. Biol.* 364 (2006) 266–274.